



Universiteit
Leiden
The Netherlands

Multimodality imaging in metabolic heart disease

Ng, A.

Citation

Ng, A. (2021, March 23). *Multimodality imaging in metabolic heart disease*. Retrieved from <https://hdl.handle.net/1887/3157141>

Version: Publisher's Version

License: [Licence agreement concerning inclusion of doctoral thesis in the Institutional Repository of the University of Leiden](#)

Downloaded from: <https://hdl.handle.net/1887/3157141>

Note: To cite this publication please use the final published version (if applicable).

Cover Page



Universiteit Leiden



The handle <https://hdl.handle.net/1887/3157141> holds various files of this Leiden University dissertation.

Author: Ng, A.

Title: Multimodality imaging in metabolic heart disease

Issue Date: 2021-03-23



Multimodality Imaging in Diabetic Heart Disease

Arnold C.T. Ng, Victoria Delgado, Roxanna Djaberi, Joanne D. Schuijf,
Mark J. Boogers, Dominique Auger, Matteo Bertini, Albert de Roos,
Rutger W. van der Meer, Hildo J. Lamb, Jeroen J. Bax

Curr Probl Cardiol. 2011;36(1):9-47

ABSTRACT

Diabetic heart disease is currently defined as left ventricular dysfunction that occurs independently of coronary artery disease and hypertension. Its underlying etiology is likely to be multifactorial, acting synergistically together to cause myocardial dysfunction. Multimodality cardiac imaging such as echocardiography, nuclear, computed tomography and magnetic resonance imaging can provide invaluable insight into different aspects of the disease process, from imaging at the cellular level for altered myocardial metabolism to microvascular and endothelial dysfunction, autonomic neuropathy, coronary atherosclerosis, and finally interstitial fibrosis with scar formation. Furthermore, cardiac imaging is pivotal in diagnosing diabetic heart disease. Thus, the aim of the present review is to illustrate the role of multimodality cardiac imaging in elucidating the underlying pathophysiological mechanisms of diabetic heart disease.

INTRODUCTION

Diabetes mellitus is the most common endocrine disease in the world. Recent estimates from the World Health Organization indicate that more than 170 million people worldwide have diabetes, and that number is projected to increase to more than 360 million by the year 2030.^{1,2} Diabetic patients are at an increased risk of developing cardiovascular disease,³ and can develop heart failure independent of myocardial ischemia.⁴ Similarly, the incidence of diabetes is also increased in patients with heart failure.^{5,6} Epidemiological studies have established diabetes as an independent risk factor for developing heart failure, even after correcting for the presence of coronary artery disease.^{3,4,7} Since it was first described by Rubler et al. more than 3 decades ago,⁸ diabetic cardiomyopathy is currently defined as left ventricular (LV) dysfunction that occurs independently of significant coronary artery disease and hypertension.⁹ However, the clinical spectrum of diabetes and heart failure is wide, ranging from subclinical disease to overt clinical heart failure. Thus, the term diabetic cardiomyopathy is usually reserved for diabetic patients with overt myocardial dysfunction with signs and symptoms of congestive heart failure.⁸ In contrast, diabetic heart disease is a better description for diabetic patients with evidence of subclinical myocardial dysfunction without overt heart failure symptoms.

Various mechanisms underlie the etiology of diabetic heart disease, including processes such as altered myocardial metabolism with subsequent steatosis and lipotoxicity, endothelial dysfunction with microvascular disease, autonomic neuropathy, altered myocardial structure with fibrosis and atherosclerosis.¹⁰ Often, these processes are not mutually exclusive, but act synergistically together and result in myocardial dysfunction. Multimodality imaging such as echocardiography, nuclear imaging, computed tomography (CT) and magnetic resonance imaging (MRI) can all reveal different etiological aspects of diabetic heart disease (Table 1). The present manuscript will illustrate the role of multimodality cardiac imaging in elucidating the pathogenesis of diabetic heart disease, starting from imaging at the cellular level for altered myocardial metabolism to microvascular and endothelial dysfunction, autonomic neuropathy, coronary atherosclerosis, and finally interstitial fibrosis with scar formation. Furthermore, features of myocardial diastolic and systolic dysfunction that are consequent to these pathophysiological processes will also be examined.

Table 1. Pathogenesis of diabetic heart disease and the applications of multimodality imaging in elucidating the underlying mechanisms

Altered metabolism

Magnetic resonance spectroscopy

Endothelial dysfunction and microvascular disease

Flow mediated dilatation

Stress echocardiography

Myocardial contrast echocardiography

Nuclear myocardial perfusion imaging

Positron emission tomography

Contrast-enhanced magnetic resonance imaging

Cardiac autonomic dysfunction

123-iodine metaiodobenzylguanidine (¹²³I MIBG) SPECT

Positron emission tomography

Coronary atherosclerosis

Coronary artery calcium scoring

Coronary CT angiography

Myocardial structural changes with fibrosis

Echocardiographic intergrated backscatter

Magnetic resonance imaging

SPECT: single photon emission computed tomography; CT: computed tomography

A) IMAGING THE PATHOGENESIS OF DIABETIC HEART DISEASE

1. Altered metabolism

Increasingly, evidence is emerging that diabetic patients have myocardial functional and structural changes that are independent of coronary artery disease or hypertension.⁹⁻¹¹ Although the mechanisms leading to diabetic heart disease are complex and not fully understood, one of the pathophysiological causes is the excessive fatty acid accumulation within organs such as the heart (known as steatosis), eventually leading to irreversible cellular death through complex mechanisms (also known as lipotoxicity).¹²⁻¹⁴

Under physiological conditions, fatty acids are normally absorbed through the intestines and are mostly stored as triglycerides within adipocytes with minimal accumulation within other tissues such as the heart. However, increased nutritional fatty acid intake and increased lipolysis in diabetes or obesity will lead to increased free fatty acid delivery to non-adipose tissues.¹³⁻¹⁵ When the amount of free fatty acids uptake by the heart exceeds its oxidative capacity, excessive fatty acids will be stored as triglycerides within the myocyte cytoplasm. However, part of the fatty acid is redirected into non-oxidative

pathways giving rise to toxic fatty acid intermediates such as ceramide. These toxic fatty acid intermediates disrupt normal cellular signalling and alter myocyte function and structure by complex mechanisms, eventually leading to cellular apoptosis and replacement fibrosis. Thus, it is currently accepted that intracellular triglycerides are probably inert, but are reflective of the increased intracellular concentrations of toxic fatty acid intermediates. At present, myocardial triglycerides can be quantified by using hydrogen 1 magnetic resonance spectroscopy (^1H MRS).¹⁶

Magnetic resonance spectroscopy. Currently, ^1H MRS can be performed using MR systems with a high field strength (1.5 Tesla or above). Often, cardiac and respiratory motion triggering are employed to improve the reliability and spectral quality of myocardial ^1H MRS by reducing cardiac and respiratory motion artefacts, and reduce the chance of contamination by signals arising from the epicardial fat.¹⁷ A typical myocardial ^1H MR spectrum will display signals arising from water, creatine, choline and fat (Figure 1). As the water signal is approximately 100-1000 times that of the fat signal, acquisition of ^1H MR spectra both with and without water suppression is essential for reliable quantification of intramyocardial triglyceride content. Using dedicated software, signal amplitudes from the intracellular triglycerides and water are quantified and expressed as triglyceride/water ratio.

Several studies have utilized ^1H MRS to relate myocardial triglyceride content and LV function in healthy volunteers, and in obese and diabetic patients.^{16, 18-22} It is known that myocardial triglyceride content increases with normal physiological aging, and is inversely correlated with the age-related decline in myocardial function.²¹ Similarly, myocardial triglyceride content is increased in obese and diabetic patients.^{19, 20, 23} Furthermore, the accumulation of myocardial triglyceride was associated with myocardial dysfunction in these patients. These findings are in agreement with experimental animal studies showing direct toxic effects of fatty acid intermediates on the myocardium.^{24, 25}

Several human studies have examined the reversibility of myocardial dysfunction associated with steatosis. Both Hammer et al. and Schrauwen-Hinderling et al. have demonstrated that weight loss was able to partially reverse myocardial triglyceride accumulation in diabetic and obese patients respectively, and this was associated with improvements in LV function.^{18, 26} In contrast, there is currently conflicting evidence on the role of medications in reducing intramyocardial triglyceride accumulation.^{22, 27} For example, Zib and co-workers demonstrated that pioglitazone (a thiazolidinedione which increases whole-body insulin sensitivity) significantly reduced myocardial and hepatic triglyceride contents, but there were no significant changes in LV mass and ejection fraction (EF).²⁷ On the other hand, van der Meer and co-workers demonstrated

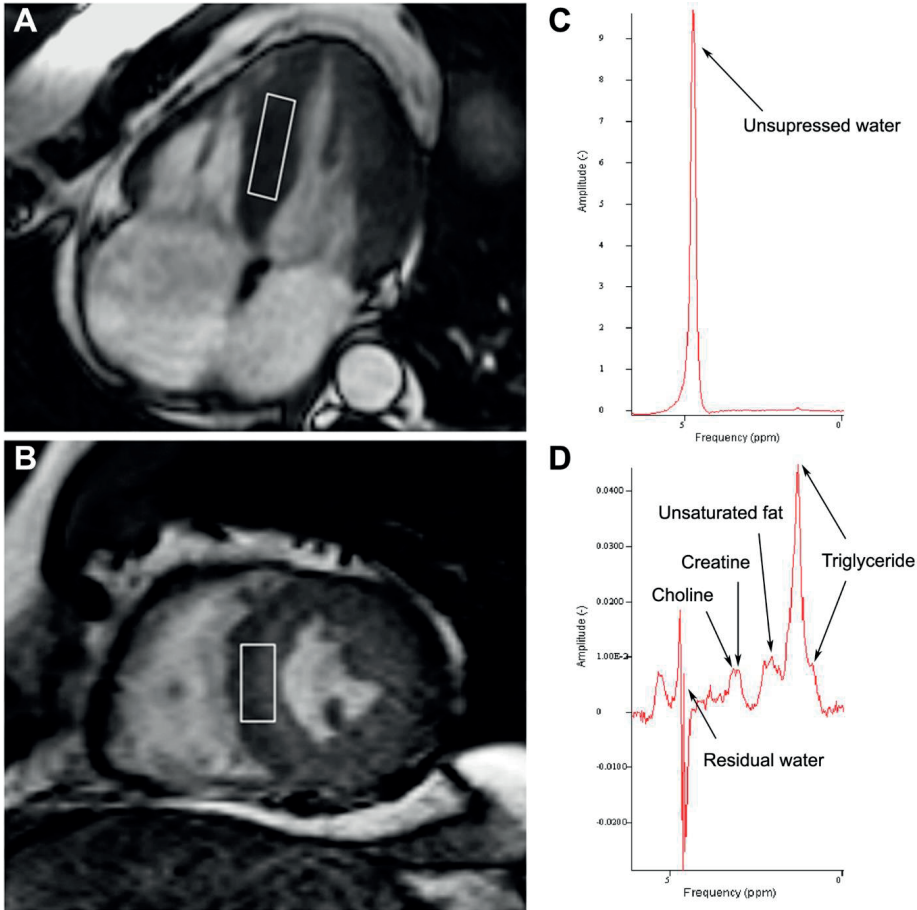


Figure 1. Examples of image acquisition and spectra from a patient. Panel A and B: 4-chamber and short axis views with the volume of interest placed in the interventricular septum; Panel C: Typical unsuppressed spectrum showing the water peak; Panel D: Typical water-suppressed spectrum showing the various peaks from triglyceride, unsaturated fat, creatine and choline. The amplitudes of the spectra are in arbitrary units, and concentrations of triglyceride are usually expressed as a ratio relative to the peak water amplitude.

significant improvement in LV diastolic function in diabetic patients treated with pioglitazone, but myocardial triglyceride content remained unchanged.²² Future studies are clearly needed to further investigate the role of medications in reversing myocardial steatosis. However, as previously noted, intracellular triglycerides are probably inert, and the relationship between myocardial triglyceride accumulation and LV dysfunction likely represents an association rather than a causal relationship. Furthermore, there is currently no evidence to suggest that myocardial triglyceride accumulation will eventually result in clinical heart failure.

2. Endothelial dysfunction and microvascular disease

One of the mechanisms underlying diabetic cardiomyopathy is the presence of endothelial dysfunction and microvascular disease. The normal function of endothelial cells is to maintain vascular homeostasis in order to ensure adequate blood flow and nutrient delivery to tissues while preventing thrombosis and leukocyte diapedesis.²⁸ This is performed through the competing and opposing synthesis and release of nitric oxide (which causes smooth muscle relaxation and vasodilatation) and vasoconstrictor prostanoids and endothelin (which results in vasoconstriction). Endothelial-derived nitric oxide protects against atherosclerosis by preventing platelet and leukocyte adhesion to the vascular wall, and inhibition of smooth muscle cell proliferation.²⁹⁻³¹ Reduction or loss of endothelial nitric oxide availability results in monocyte and vascular smooth muscle cell migration into the vascular intima layer and the formation of macrophage foam cells, the initial stages of atherosclerosis.³² In diabetic patients, the associated hyperglycemia, increased circulating free fatty acids levels and insulin resistance lead to increased mitochondrial superoxide generation, reduced endothelial nitric oxide production with reciprocal increase in vasoconstrictor prostanoids and endothelin syntheses. This will eventually result in endothelial dysfunction and atherosclerosis.^{32,33} Furthermore, dysregulation of vascular smooth muscle function is exacerbated by impairments in sympathetic nervous system function, as is often seen in diabetic autonomic neuropathy (see below).³⁴ Various imaging techniques such as flow mediated dilatation (FMD), stress echocardiography, myocardial contrast echocardiography, nuclear perfusion imaging, positron emission tomography (PET) and contrast-enhanced MRI may be employed to evaluate endothelial function and microvascular disease.

Flow mediated dilation. FMD of the brachial artery provides a non-invasive estimation of systemic endothelial function.³⁵ In this method, the brachial artery diameter is measured using B-Mode ultrasound or a wall-tracking system, before and after an increase in shear stress that is induced by reactive hyperemia. FMD is thus defined as the percentage change in diameter of the brachial artery and measures the function of endothelium dependent vasodilatation (Figure 2). The observed brachial artery dilatation has been shown to be closely related to coronary endothelial function and vasoreactivity.³⁶

FMD has been widely used in research to study the natural course of endothelial function with age and its role in the initiation and progression of vascular disease.³⁷ For example, FMD ranges from approximately 20% in young adults to 0% in patients with established CAD, while mean FMD values were also reduced (range 0-12%) in diabetic patients.³⁸ Often, diabetic patients may show evidence of myocardial perfusion defects without a corresponding obstructive epicardial coronary artery disease, suggestive of endothelial dysfunction with microvascular disease.³⁹ Accordingly, a recent study demonstrated a

significant lower FMD in diabetic patients with perfusion defects compared to those without perfusion defects on single photon emission computed tomography (SPECT) (FMD $3.6 \pm 2.4\%$ vs. $6.4 \pm 2.6\%$, $p < 0.001$), despite the absence of obstructive coronary disease.⁴⁰ This observation emphasizes the potential role of endothelial dysfunction and corresponding microvascular disease on myocardial perfusion in diabetic patients.

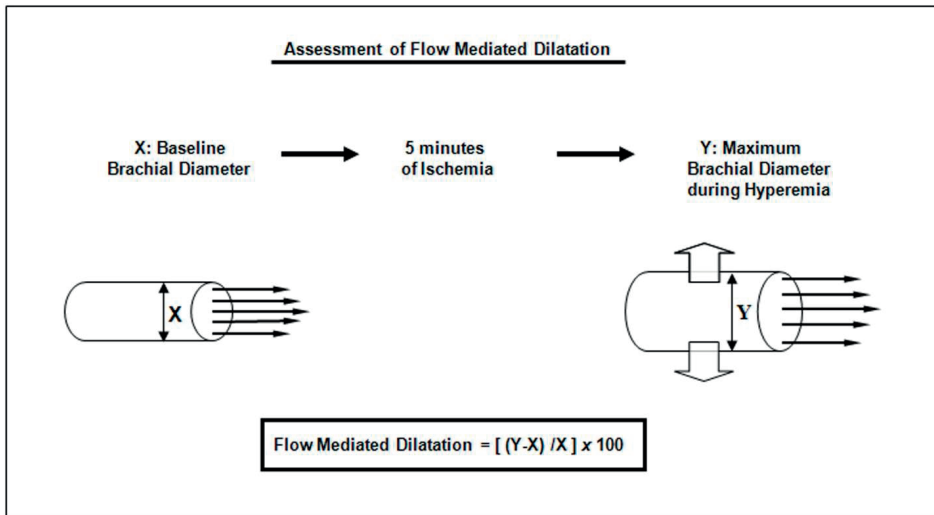


Figure 2. Assessment of flow mediated dilatation. The brachial artery is visualized distal to the elbow using ultrasonography. Next, ischemia is induced in the forearm distal to the location of the transducer by inflating a blood pressure cuff for 5 minutes at a pressure of at least 200 mmHg. After cuff deflation, ultrasonography is continued for 5 minutes with measurements at approximately 30-second intervals. Widest lumen diameter is used as maximal vasodilation achieved during reactive hyperemia. Flow mediated dilatation is expressed as the percentage change relative to the baseline diameter.

Detection of microangiopathy by stress echocardiography. Previous echocardiographic studies have also evaluated the relationship between myocardial blood flow and LV systolic and diastolic dysfunction in diabetic patients.^{41,42} Fang et al. evaluated 41 diabetic patients with normal resting LVEF and without coronary artery disease as demonstrated by a normal dobutamine stress echocardiography.⁴¹ Systolic myocardial velocity (Sm) was measured at rest and at peak dobutamine dose with color-coded tissue Doppler imaging. Compared to healthy controls, diabetic patients showed significantly reduced resting Sm (4.2 ± 0.9 cm/s vs. 4.7 ± 0.9 cm/s, $p = 0.012$). At peak dobutamine dose, Sm increased in diabetic patients and controls reaching comparable values (8.9 ± 1.8 cm/s vs. 9.6 ± 2.1 cm/s, $p =$ not significant).⁴¹ Therefore, this normal response to stress suggested that ischemic etiology might not be a cause for the resting left ventricular systolic dysfunction. These results were later confirmed by another study from the same group using myocardial contrast echocardiography to assess myocardial blood flow.⁴²

Detection of microangiopathy by myocardial contrast echocardiography. Echocardiographic microbubble contrast agents are normally used for LV opacification to enhance endocardial border detection, thus improving the accuracies of LV volume quantification and wall motion analyses. In addition, the microbubble contrast agents also permit evaluation of myocardial perfusion and myocardial blood flow.⁴³ As these microbubble contrast agents have similar microvascular rheology as red blood cells, they stay within the intravascular compartment. Using a low mechanical index during imaging, these microbubbles resonate and appear bright on echocardiography. When a high mechanical index ultrasound pulse is transmitted, the microbubbles are destroyed within the myocardium, thereby reducing the myocardial contrast intensity to nearly zero. The rate of replenishment within the myocardium is thus dependent on the presence of intact microvasculature and myocardial blood flow rate, and the intensity at which the contrast effect plateaus is dependent on myocardial blood volume. Thus, normally perfused myocardium appears as enhanced myocardium, whereas those areas with impaired perfusion appear as dark or patchy areas (Figures 3A and 3B).

In a study by Moir and co-workers who recruited 26 healthy controls and 22 type 2 diabetic patients with normal LVEF and absent coronary artery disease, the relationship between myocardial flow reserve post-stress and myocardial function was explored.⁴² Myocardial blood flow and function were quantified by myocardial contrast echocardiography and tissue Doppler strain/strain rate imaging respectively. Compared to controls, resting longitudinal peak systolic strain ($-14.4 \pm 4.6\%$ vs. $-18.7 \pm 3.1\%$, $p = 0.006$) was significantly lower in diabetic patients, but resting myocardial blood flow was comparable (5.1 ± 3.5 vs. 4.6 ± 3.2 , $p = 0.62$). Post-stress, myocardial blood flow reserve was significantly lower in diabetic patients (2.4 ± 1.0 vs. 3.8 ± 2.1 , $p = 0.01$). However, there was no correlation between myocardial blood flow reserve and resting myocardial function (Figure 3C). Thus, the authors concluded that although subclinical myocardial dysfunction and microvascular disease may coexist, it may not be the sole causative factor in diabetic heart disease.

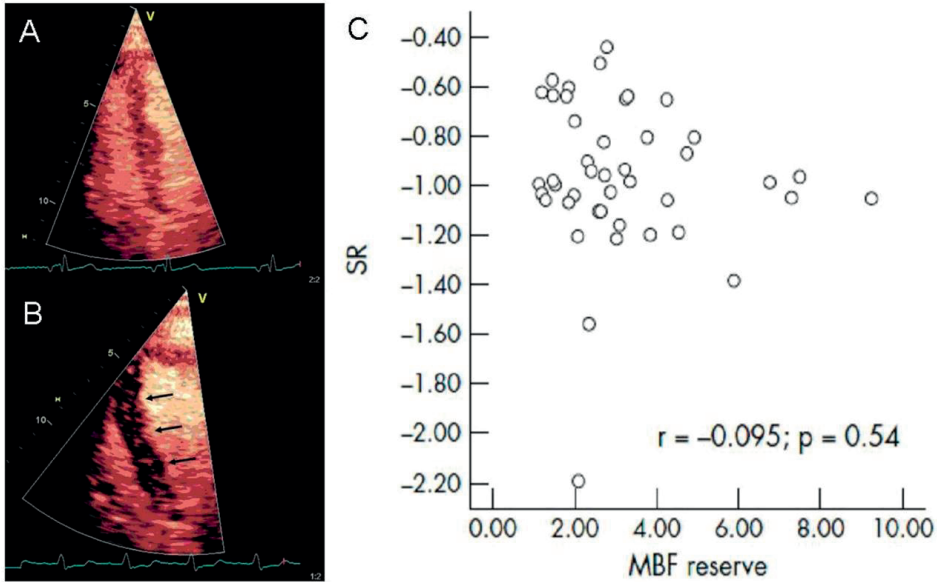


Figure 3. Examples of myocardial contrast echocardiography assessing myocardial blood flow. After a high mechanical index ultrasound pulse, the microbubbles are initially destroyed before returning to reperfuse the myocardium. Areas with normal myocardial blood flow show a homogeneous replenishment of the myocardium (panel A). In contrast, areas with impaired perfusion appear as dark patchy, non-replenished areas (arrows, panel B). In diabetic cardiomyopathy, myocardial blood flow reserve post-stress did not correlated with resting myocardial function as assessed by tissue Doppler strain rate imaging (panel C).

SR: strain rate; MBF: myocardial blood flow. Adapted with permission from Moir et al. *Heart* 2006;92:1414–1419.

Nuclear myocardial perfusion imaging. Myocardial perfusion imaging by thallium-201 or technetium-99m sestamibi SPECT is a widely used and validated non-invasive tool for the diagnosis of myocardial ischemia. ECG-gated SPECT allows both quantitative evaluation of cardiac function and myocardial perfusion to detect ischemia during exercise testing or pharmacological stress with adenosine, dipyridamole or dobutamine (Figure 4).⁴⁴ The presence of myocardial perfusion defects during stress is due to heterogeneous flow distribution as a result of two potential mechanisms: obstructive epicardial coronary artery disease due to atherosclerosis and subsequently reduced flow during stress;⁴⁵ or insufficient vasomotor response in the coronary microvasculature due to endothelial dysfunction resulting in relative hypoperfusion during stress.⁴⁶

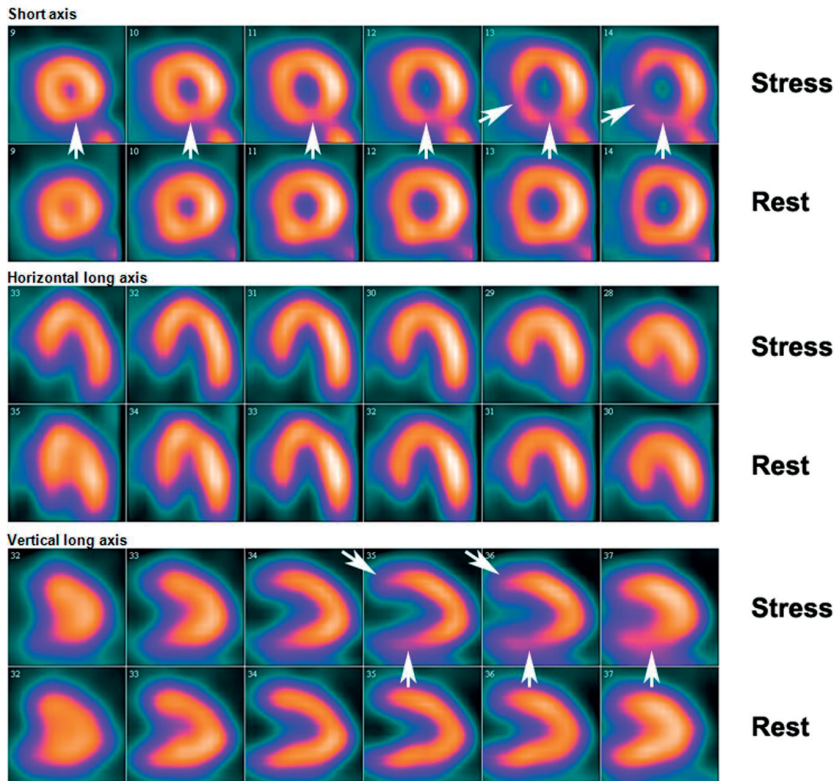


Figure 4. Myocardial perfusion using gated SPECT at rest and after adenosine stress. Resting images and stress images in the short axis, horizontal and vertical long axes are depicted. In the current example, no persistent perfusion defects were observed. Reversible perfusion defects were observed in the inferior, inferoseptal, anterior and anteroseptal regions (arrows).

The prevalence of myocardial perfusion defects as assessed by SPECT myocardial perfusion imaging in asymptomatic diabetic patients ranges from 20 – 40% in several prospective studies,⁴⁷⁻⁴⁹ and the prognostic value of SPECT myocardial perfusion imaging in diabetic patients has been confirmed in several previous studies.⁴⁸⁻⁵⁰ For example, in a large cohort of 1271 diabetic patients, Kang et al. described a favorable cardiovascular prognosis in patients with a normal myocardial perfusion SPECT study (coronary event rates 1-2% per year), which increases to 3 – 4% per year in patients with mild perfusion defects, to > 7% per year for patients with moderate to severe perfusion defects. The incremental cardiovascular predictive value of SPECT in diabetic patients has been attributed to both the direct detection of underlying obstructive epicardial coronary disease, and its ability to reflect on endothelial dysfunction within the coronary microvasculature.⁵¹

It has been previously shown that coronary endothelial dysfunction is a precursor to overt atherosclerosis and is reversible to a certain extent, such as with statin therapies.^{52, 53} Accordingly, in the Detection of Ischemia in Asymptomatic Diabetics (DIAD) study, inducible myocardial ischemia at baseline was shown to resolve in up to 79% of asymptomatic patients with diabetes at 3 years follow-up.⁵⁴ This resolution was suggested by the authors to be secondary to improvements in endothelial dysfunction and stabilization of atherosclerotic plaques as a result of treatment with statins, aspirin and angiotensin-converting enzyme inhibitors.

Positron emission tomography. Although SPECT imaging is routinely used in the clinical setting, image quality may be suboptimal in obese and female diabetic patients due to attenuation artifacts. As such, assessment of myocardial perfusion by PET may be a good alternative in situations where SPECT imaging quality is suboptimal.⁵⁵ Myocardial perfusion imaging by PET uses high energy gamma photons produced by positron-emitting radionuclides, and has superior spatial resolution compared to conventional SPECT.⁵⁶ By combining readily available attenuation correction algorithms for photon attenuation, scatter and random events, PET imaging can provide a truly quantitative measure of myocardial blood flow (in ml/min/g) and coronary flow reserve in absolute terms.⁵⁷⁻⁵⁹ Thus far, this technique has been applied in research to examine coronary microvascular reactivity in various study populations.⁶⁰⁻⁶⁴ Several studies have demonstrated dysregulation of myocardial microvascular reactivity in diabetic patients.⁶²⁻⁶⁴ For example, Kjaer and co-workers demonstrated endothelial dysfunction using ¹³N-ammonia PET imaging in type 2 diabetic patients without evidence of epicardial coronary disease compared to normal controls.⁶² Similarly, Prior and co-workers demonstrated a significantly lower total vasodilator capacity in normotensive diabetic (-17%) and hypertensive diabetic (-34%) patients compared to insulin sensitive individuals.⁶⁴

Magnetic resonance perfusion imaging. In MRI, myocardial perfusion imaging relies on the injection of a gadolinium-based paramagnetic contrast agent which alters the relaxation properties of the proton nuclei in its vicinity. The subsequent transit of the contrast agent through the cardiovascular system and into the myocardium can be detected using pulse sequences which focus on T₁ weighted images (Figure 5). Thus, using dipyridamole as a pharmacological stressor, magnetic resonance perfusion imaging allows non-invasive quantification of myocardial perfusion during baseline conditions and during maximal hyperemia.

There are currently a limited number of studies that have assessed MRI myocardial perfusion imaging in diabetic patients. In a small study by Taskiran et al., 19 type 1 diabetic patients were compared against 10 healthy controls.⁶⁵ All the diabetic patients had no

major microvascular disease, and were divided into the presence or absence of autonomic neuropathy. After induction of maximal hyperemia by dipyridamole, myocardial perfusion index was significantly lower in diabetic patients with autonomic neuropathy compared to those without neuropathy or normal controls ($p < 0.001$). Thus, altered myocardial perfusion associated with autonomic neuropathy may be a potential pathophysiological mechanism underlying the increased mortality observed in diabetic patients.

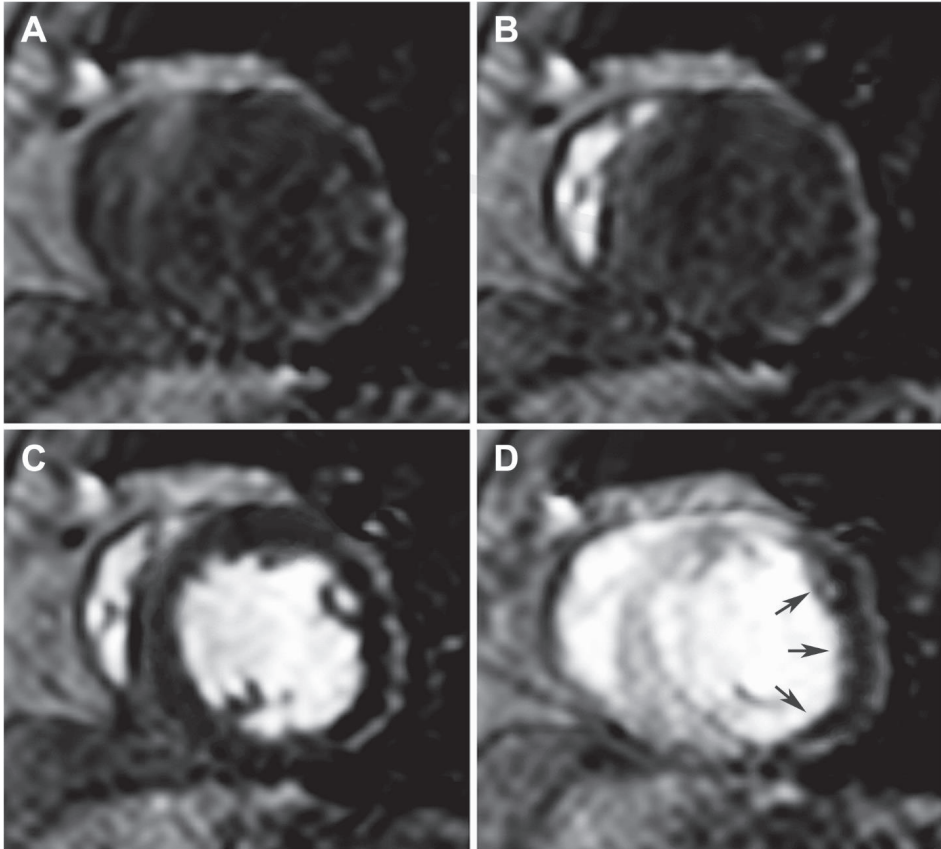


Figure 5. Example of myocardial perfusion imaging by magnetic resonance imaging during the first pass of an intravenously injected contrast bolus. Prior to contrast injection, the blood pool, right and left ventricular myocardium are dark (Panel A). Following contrast injection, contrast enhancement is then first observed in the right ventricular cavity (Panel B), followed by the left ventricular cavity (Panel C), and finally followed by enhancement of the myocardium (Panel D). The present patient had a large perfusion defect in the posterolateral wall (arrows).

3. Cardiac autonomic dysfunction

Diabetic neuropathies are a heterogeneous group of diabetic complications that affects different parts of peripheral nervous system. Its pathophysiology is likely to be multifactorial, involving alterations in metabolism, micro- and macrovascular dysfunction, deficiency of neurohormonal growth factor and autoimmune nerve damage.⁶⁶ Although diabetic autonomic neuropathy can affect every system in the body, cardiac autonomic neuropathy (CAN) is particularly associated with an increased risk of silent myocardial infarction and sudden cardiac death, thus contributing to significant cardiovascular morbidity and mortality.⁶⁷ The prevalence of CAN in type 2 diabetic patients is estimated to be around 20 – 30% of patients.⁶⁸ Clinical manifestations of CAN include the presence of resting tachycardia (heart rate > 100 beats/min), postural hypotension (fall in systolic blood pressure > 20mmHg or diastolic blood pressure > 10mmHg upon standing) without an appropriate reflex increase in heart rate, exercise intolerance due to blunting of cardiac output in response to exercise, or silent myocardial infarction.^{69, 70}

The presence of CAN conveys a poor clinical outcome. Previous meta-analysis by Vinik and co-workers assessed the prognostic value of CAN in diabetic patients.⁷⁰ Using the pooled analyses from 12 studies involving a total of 1486 study subjects, they estimated that the pooled prevalence rate risk for silent myocardial infarction in diabetic patients was 1.96 (95% confidence interval 1.53 – 2.51, $p < 0.001$).⁷⁰ In the same review, the pooled estimate of the relative risk for mortality, based on 15 studies with 2900 patients, was 2.14 (95% confidence interval 1.83 – 2.51, $p < 0.0001$) for diabetic patients with CAN. Thus, it was estimated that the 5 year mortality rate is 5 times higher in diabetic patients with CAN compared to patients without evidence of CAN.^{69, 70} Therefore, early diagnosis and recognition of CAN is crucial as it may impact on the clinical decision making of these patients.

Diagnosis of CAN involves assessment of both parasympathetic and sympathetic nervous system using a range of different tests. Assessment of parasympathetic nervous system includes the resting heart rate, beat-to-beat variation with deep breathing (E:I ratio), 30:15 heart rate ratio with standing, Valsalva ratio, and spectral analysis of heart rate variation.⁶⁹ Assessment of sympathetic nervous system includes the resting heart rate, spectral analysis of heart rate variation, postural blood pressure, hand grip blood pressure, cold pressor response, sympathetic skin galvanic response, sudorometry, and cutaneous blood flow.⁶⁹ However, all these tests are indirect assessments of the autonomic nervous system and are less sensitive than direct assessments by cardiac radionuclide imaging with SPECT or PET.^{71, 72}

Currently, SPECT and PET imaging are available for the assessment of cardiac sympathetic adrenergic innervation and activation.⁷²⁻⁷⁴ Essentially, adrenergic nerve imaging is based on two principles; synthesis of false neurotransmitters (catecholamine analogs) or the labeling of true adrenergic neurotransmitters. Both techniques allow evaluation of abnormalities in cardiac sympathetic innervation by visualizing the uptake and storage of radiolabeled neurotransmitters transported into the presynaptic nerve terminals.

123-iodine metaiodobenzylguanidine (¹²³I MIBG) SPECT. Abnormalities in sympathetic innervation can be assessed using 123-iodine metaiodobenzylguanidine (¹²³I MIBG), a norepinephrine analog that is taken up and accumulated in the presynaptic nerve terminals.^{68, 75, 76} Currently, ¹²³I MIBG represents the most commonly used tracer in clinical cardiology to evaluate cardiac sympathetic innervation patterns.⁷⁶ Planar and tomographic SPECT images are acquired 10-20 minutes (early) or 3-4 hours (late) after MIBG administration. From the planar images, semi-quantitative measurements such as heart-to-mediastinum (H/M) ratio and cardiac washout rate are used to evaluate global sympathetic innervation. SPECT images are used to assess regional abnormalities in sympathetic innervation as depicted in Figure 6. At present, several studies using ¹²³I MIBG imaging have demonstrated the presence of global and regional abnormalities in sympathetic innervation in diabetic patients.^{68, 75, 77} Turpeinen and co-workers performed ¹²³I MIBG scintigraphy to evaluate regional abnormalities in sympathetic innervation pattern in 7 type 1 and 13 type 2 diabetic patients.⁷⁷ Type 2 diabetic patients showed reduced ¹²³I MIBG uptake in the inferoposterior segments compared to type 1 diabetic patients. However, conventional indirect measures of autonomic function by power spectral analysis of heart rate variability failed to detect any differences between the 2 groups.

Nagamachi and co-workers subsequently evaluated the prognostic value of cardiac MIBG imaging by retrospectively evaluating 144 type 2 diabetic patients for the occurrence of cardiac events (arrhythmia, heart failure or acute myocardial infarction), and all-cause mortality.⁶⁸ After a mean follow-up period of 7.2 ± 3.2 years, 17 (11.8%) patients experienced a cardiac event, of which 7 died. An additional 9 patients died due to non-cardiac causes. On multivariate analysis, the presence of CAN (relative risk 6.75, 95% confidence interval 1.16 – 39.3, $p = 0.03$) was an independent predictor of cardiac events on follow-up. Similarly, the presence of CAN (relative risk 17.1, 95% confidence interval 1.07 – 27.9, $p = 0.04$) and a reduced H/M ratio on delayed ¹²³I MIBG imaging (relative risk 6.0, 95% confidence interval 1.18 – 30.6, $p = 0.04$) were independent predictors of all-cause mortality.

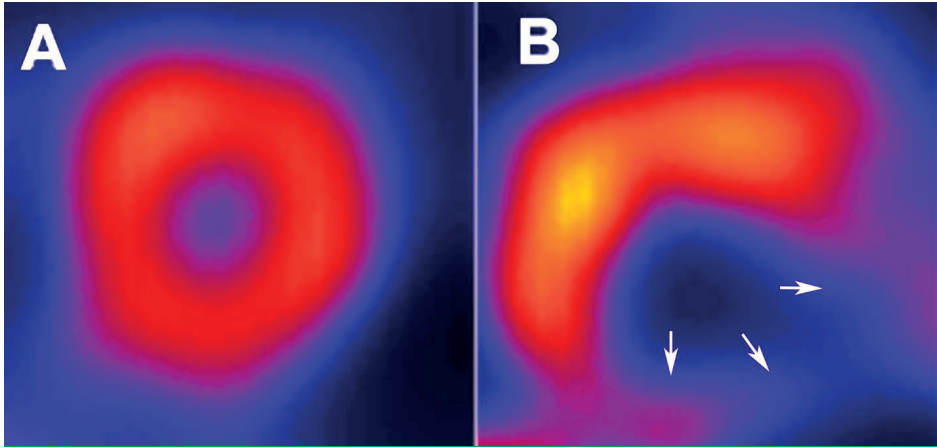


Figure 6. Sympathetic innervation as assessed with ^{123}I MIBG SPECT imaging. Panel A: Example of a patient with normal sympathetic innervation on ^{123}I MIBG SPECT imaging. Panel B: Example of a patient with regional abnormalities as assessed with ^{123}I MIBG SPECT imaging (arrows).

Positron emission tomography. PET imaging is the only technique that permits absolute quantification of myocardial sympathetic innervation pattern. Using carbon-11 methoxyephedrine (^{11}C HED) in PET imaging has the advantage of accurately detecting regional abnormalities in sympathetic innervation. Stevens and co-workers evaluated regional abnormalities in cardiac sympathetic innervation with ^{11}C HED PET imaging in 29 diabetic patients and compared to 10 healthy subjects.⁷² The diabetic patients were categorized into the presence of mild or severe diabetic autonomic neuropathy. Using the absolute difference in tracer uptake of the myocardium, the extent of regional sympathetic denervation was expressed as the percentage of the LV in all subjects with diabetes. The study showed that the extent of regional sympathetic denervation was significantly larger in patients with severe autonomic neuropathy as compared to patients with mild autonomic neuropathy ($48 \pm 19\%$ vs. $6 \pm 5\%$, $p < 0.01$). Furthermore, there was evidence of sympathetic dysinnervation with increased innervation in the basal myocardial segments but decreased innervation in the apical myocardial segments (Figure 7). Thus, this observed regional myocardial variation in sympathetic innervation and could contribute to myocardial electrical instability and potentially life-threatening arrhythmias.

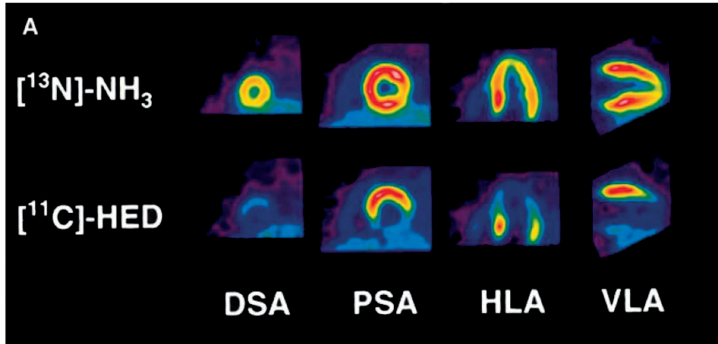


Figure 7. PET imaging of a patient with severe diabetic autonomic neuropathy. Top row: short and long axis images of the left ventricle showing normal blood flow as indicated by homogenous ^{13}N NH_3 tracer uptake. Bottom row: extensive abnormalities in ^{11}C HED PET imaging. The basal myocardial segments showed excessively high ^{11}C HED retention suggestive of increased innervation, whereas there was decreased innervation in the apical myocardial segments as demonstrated by absent tracer uptake. Adapted with permission from Stevens et al., *J Am Coll Cardiol* 1998;31:1575-1584.

4. Coronary atherosclerosis

As previously alluded to, the presence of microvascular disease and endothelial dysfunction in diabetic patients are often the precursors of vascular atherosclerosis. Although the presence of significant coronary stenosis will result in myocardial dysfunction and is thus strictly not considered as “diabetic heart disease”, its prevalence in diabetic patients is higher than non-diabetics, and is associated with significant cardiovascular morbidity and mortality.⁷⁸ Furthermore, the presence of coronary atherosclerosis without significant luminal narrowing may not be entirely benign.⁷⁹ Indeed, previous studies have demonstrated that myocardial infarction and unstable angina are frequently caused by coronary lesions deemed to be non-significant prior to the event.^{80, 81} Thus, it may be useful to identify and risk-stratify patients into normal coronary arteries without atherosclerosis, non-significant coronary artery disease, and significant coronary artery disease. At present, computed tomography (CT) techniques such as coronary artery calcium (CAC) scoring and coronary CT angiography (CTA) are considered the most robust imaging techniques for non-invasive visualization of coronary atherosclerosis.

Coronary artery calcium scoring. CAC score can characterize the location and burden of coronary atherosclerosis by detecting calcium present within atherosclerotic plaques. Image acquisition for CAC scoring typically involves acquiring multiple, non-contrast, thick slice images of the entire heart. Using a cut-off value of greater than 130 Hounsfield units to define calcium, coronary calcifications can be identified as bright white structures on the CT images (Figure 8).

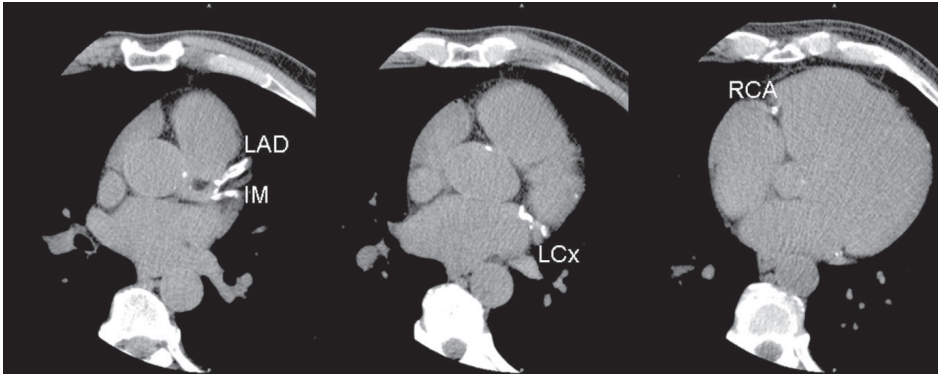


Figure 8. Example of a diabetic patient with extensive coronary calcification in all 3 coronary arteries. Total coronary calcium score was 1599. IM: intermediate branch; LAD: left anterior descending coronary artery; LCx: left circumflex artery; RCA: right coronary artery.

Semi-quantification of coronary calcium is commonly expressed by the Agatston score, which uses the plaque size, density and a weighting factor to calculate a value ranging from 0 (absence of detectable calcium) to over 1000 (indicating the presence of extensive coronary calcifications). Importantly, there is a clear relationship between the CAC score and the extent of coronary atherosclerosis, as well as the presence of significant coronary stenosis.⁸² However, the association between CAC score and extent of coronary atherosclerosis is not linear as severe coronary stenosis can occur at sites with limited calcium deposition. Likewise, extensive CAC scores can be observed in the absence of significant luminal narrowing. Thus, rather than being a diagnostic test for obstructive CAD, CAC scoring may be more valuable as a risk stratification tool to identify at-risk patients with underlying atherosclerosis who might benefit from further investigations.

In the general population, CAC scoring has indeed been shown to provide strong prognostic information. An elevated CAC score has consistently been associated with increased mortality and adverse cardiovascular events, independently of coronary risk factors.⁸³ Similar findings have been observed in diabetic patients.⁸⁴ In one of the largest series to date, Raggi et al. compared baseline CAC scores and outcomes among 9474 non-diabetic and 903 diabetic patients.⁸⁴ During a mean follow-up period of 5 years, CAC score was identified as the best predictor of all-cause mortality in both diabetic and non-diabetic individuals (Figure 9).

Moreover, further analysis revealed that for each level of CAC score, mortality was higher in diabetic patients compared to non-diabetics. Thus, CAC scoring may be a promising tool in identifying diabetic patients with increased likelihood of coronary events who might benefit from further functional evaluation and more aggressive, individually targeted preventive treatment strategies. Indeed, Anand and co-workers recently

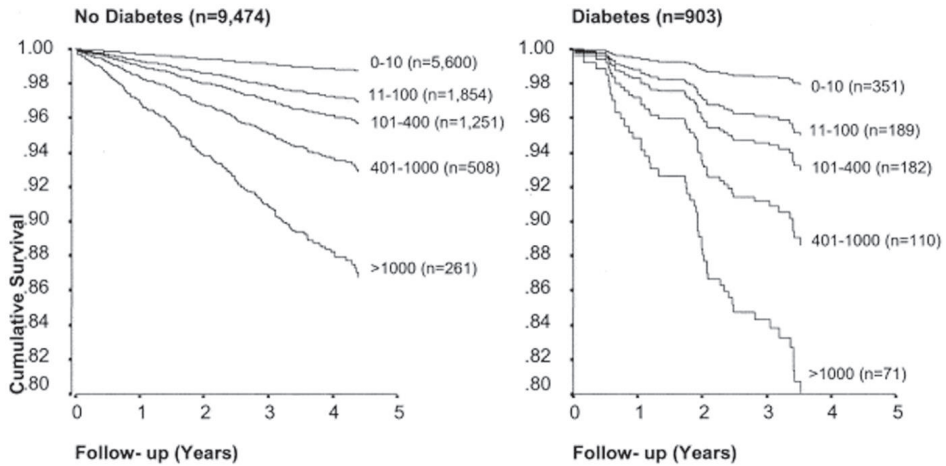


Figure 9. Cox proportional hazards survival demonstrating significantly lower survival with increasing coronary artery calcium scores by electron beam computed tomography. Comparison of survival curves show that diabetic patients have significantly lower survival with each coronary artery calcium score category compared to non-diabetic patients. Adapted with permission from Raggi et al. *J Am Coll Cardiol* 2004;43:1663-1669.

demonstrated in 510 asymptomatic type 2 diabetic patients that while the incidence of ischemia was low in patients with no or limited CAC, the likelihood of ischemia increases with higher CAC scores (Figure 10).⁸⁵

Coronary CT angiography. More detailed information on the coronary anatomy can be derived from non-invasive contrast-enhanced coronary CTA which permits direct visualization of the coronary arteries (Figure 11). Particularly with the newer generations of multi-detector row CT scanners (64-slice and higher), high sensitivities and specificities can be obtained for the detection of significant coronary stenoses. Importantly, this high diagnostic accuracy has been shown to be maintained in the presence of diabetes.^{86, 87} The advantage of this technique is the high negative predictive value which approaches 100%. Notably, coronary CTA is also unlikely to miss severe coronary artery diseases such as left main or three-vessel diseases. Moreover, this technique allows identification of coronary atherosclerotic plaques in the absence of calcium or stenosis, thus permitting visualization of early, subclinical atherosclerotic disease. To a limited extent, information on plaque composition can also be derived, although it is less precise and detailed as compared to invasive techniques such as intravascular ultrasound (IVUS) or optical coherence tomography.

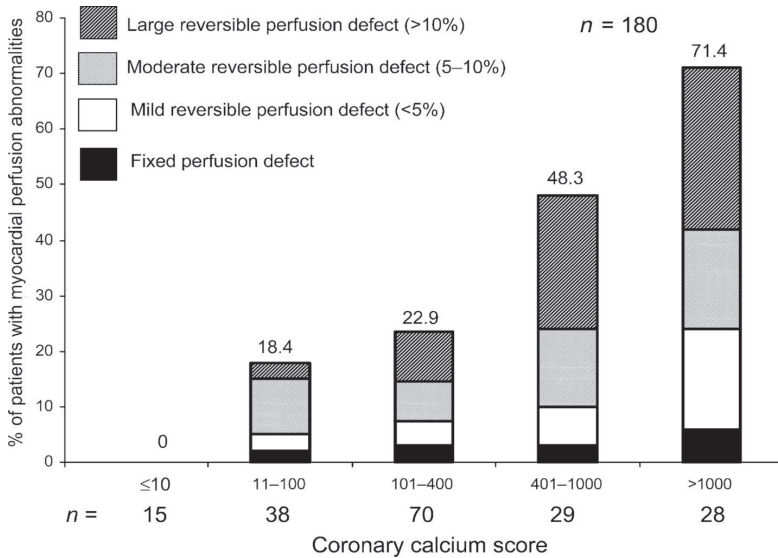


Figure 10. Relationship between the extent of coronary calcification and the prevalence/severity of myocardial perfusion abnormality. Increasing coronary artery calcium score was associated with both an increased incidence of perfusion abnormalities, and larger perfusion defects. Adapted with permission from Anand et al. *Eur Heart J* 2006;27:713-721.

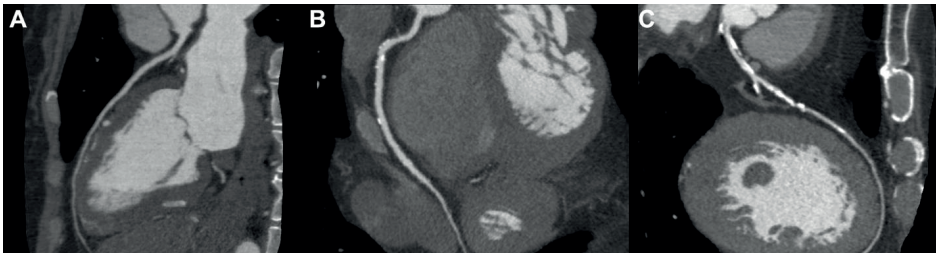


Figure 11. Evaluation of coronary artery disease with coronary CT angiography in patients with type 2 diabetes. Panel A: curved multiplanar reformation (cMPR) of the left anterior descending coronary artery without any evidence of atherosclerosis. Panel B: cMPR of the right coronary artery revealing diffuse atherosclerosis in the absence of significant stenosis. Panel C: cMPR of the left anterior descending coronary artery revealing extensive atherosclerosis with multiple significant (> 50% luminal narrowing) lesions.

Using coronary CTA, Pundziute et al. recently demonstrated that diabetic patients have more extensive, diffuse coronary atherosclerosis compared to matched non-diabetic patients.⁸⁸ Interestingly, this increased plaque burden was mainly attributable to an increased number of non-obstructive lesions, while the incidence of significant stenosis was similar amongst both populations. In a smaller population, these observations were later confirmed by the same group using MSCT and invasive plaque imaging with grey-scale and virtual histology IVUS (VH IVUS) (Figure 12).⁸⁹

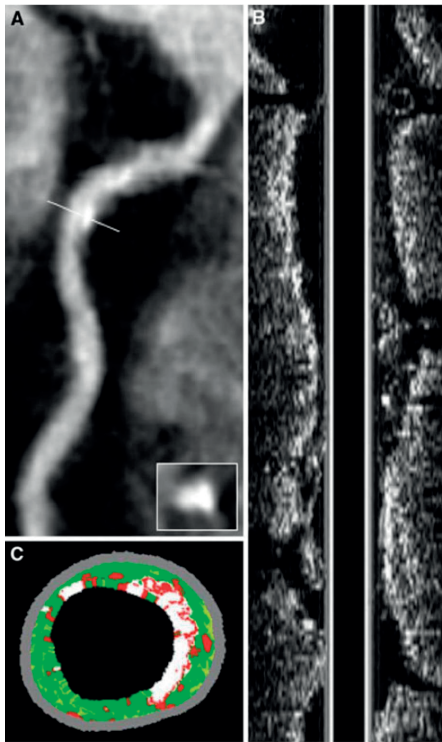


Figure 12. Example of coronary atherosclerosis in a type 2 diabetic patient as demonstrated by coronary CTA (Panel A), gray-scale intravascular ultrasound (IVUS, Panel B), and virtual histology IVUS (VH IVUS, Panel C). Panel A: Curved multiplanar reformation of the right coronary artery by CTA demonstrated diffuse atherosclerosis along the course of the artery, and a mixed plaque was observed in the proximal part of the artery in both longitudinal and transverse images. Panel B: The presence of diffuse atherosclerosis was confirmed in longitudinally reconstructed IVUS image. Panel C: Corresponding VH IVUS image at the minimal luminal area site of the atherosclerotic plaque, demonstrating the features of a fibro-calcific plaque. Fibrous areas were marked in green, fibro-fatty in yellow, calcium in white and necrotic core in red. Adapted with permission from Pundziute et al., *J Nucl Cardiol* 2009;16:376-383.

Diabetic patients had significantly higher plaque burden and more calcified lesions than non-diabetics.⁸⁹ In another study composed of 80 asymptomatic type 2 diabetic patients, Ambrose and co-workers compared CAC scoring and CTA and demonstrated that CTA may reveal substantial plaque burden even in patients with zero or low CAC scores (Figure 13).⁹⁰ Thus, coronary CTA may be more accurate in evaluating the presence and extent of coronary atherosclerosis in diabetic patients compared to CAC scoring. Preliminary results suggest that CTA has an incremental prognostic information over baseline clinical variables in both diabetic and non-diabetic patients.⁹¹

5. Myocardial structural changes with fibrosis

Although the etiology of diabetic heart disease is multifactorial, the final common pathway is accelerated myocyte apoptosis, formation of advanced glycation end-products, and development of interstitial fibrosis.⁹²⁻⁹⁴ Several animal and human studies have demonstrated increased interstitial fibrosis in diabetic patients.⁹²⁻⁹⁴ These structural changes lead to increased LV stiffness, impaired systolic and diastolic function, and ultimately the development of clinical heart failure. As such, both echocardiography and MRI can be used to detect and quantify myocardial fibrosis.

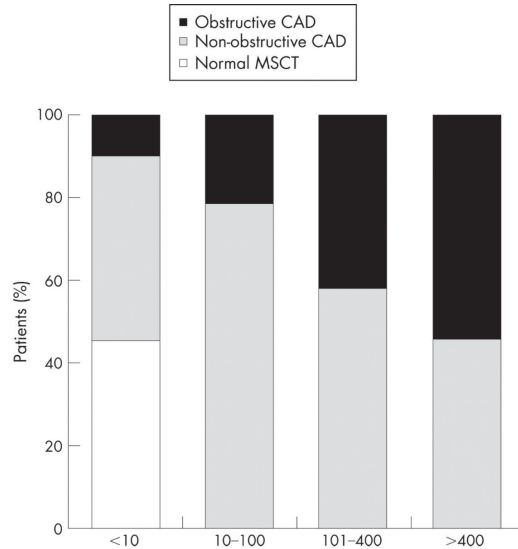


Figure 13. Bar graph demonstrating the distribution of both obstructive and non-obstructive coronary artery disease per coronary artery calcium score category in asymptomatic type 2 diabetic patients. Diabetic patients can have significant plaque burden despite zero or low (< 10) calcium score. Adapted with permission from Scholte et al. *Heart* 2008;94:290-295.

Echocardiographic integrated backscatter. Integrated backscatter analysis using 2-dimensional echocardiography has been used to non-invasively evaluate myocardial fibrosis.⁹⁵ The increased deposition of collagen alters the ultrasound reflectivity (backscattering) of the myocardial tissue and previous study has demonstrated a linear correlation between the myocardial backscatter magnitude and the amount of fibrosis content on histology.⁹⁵ The measurement of myocardial integrated backscatter is usually performed in the parasternal long-axis view by placing a region of interest in the interventricular septum and the posterior wall (Figure 14). The value of myocardial integrated backscatter obtained at end-diastole is corrected by the integrated backscatter value of the pericardium, thereby providing the calibrated integrated backscatter value.

In diabetic patients without hypertension or coronary artery disease, the myocardial ultrasound reflectivity is significantly increased compared to healthy age matched controls, suggesting the presence of increased myocardial fibrosis.⁹⁶ This observation was later confirmed by Fang and co-workers, who included 48 diabetic patients without coronary artery disease and normal LVEF, 45 diabetic patients with left ventricular hypertrophy, 45 patients with only left ventricular hypertrophy and 48 normal controls.⁹⁷ Calibrated integrated backscatter at the interventricular septum and posterior wall were significantly higher in the three groups of patients as compared to controls. Furthermore, diabetic patients with concomitant LV hypertrophy had the highest calibrated integrated

backscatter value (Figure 14). Similar trends were observed in the LV myocardial function as determined by tissue Doppler-derived strain analyses. Therefore, the presence of subclinical myocardial dysfunction in diabetic heart disease is associated with the presence of increased myocardial fibrosis. This observation of increased myocardial fibrosis was in concordance with histological studies of diabetic hearts without significant coronary disease that showed increased collagen deposition in the perivascular and interstitial regions.^{94,98,99}

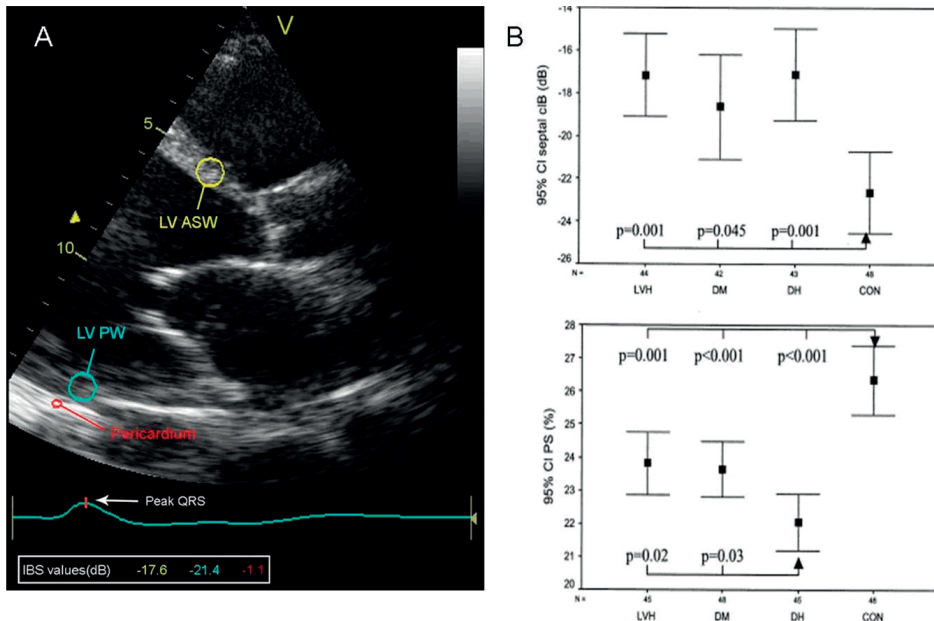


Figure 14. Evaluation of myocardial fibrosis with integrated backscatter. From LV parasternal long-axis view (panel A), the ultrasound reflectivity or integrated backscatter of the myocardium is measured at the inter-ventricular septum and posterior wall, and corrected for the pericardial integrated backscatter value. Compared to normal controls, diabetic patients and non-diabetic patients with LV hypertrophy had significantly lower longitudinal peak strain and higher myocardial integrated backscatter value. However, diabetic patients with LV hypertrophy had the highest myocardial integrated backscatter with the lowest longitudinal peak strain. PS: cIB: calibrated integrated backscatter; CON: control; DH: diabetic patients with left ventricular hypertrophy; DM: diabetic patients; LVH: patients with left ventricular hypertrophy; PS: peak strain. Adapted with permission from Fang et al. *J Am Coll Cardiol* 2003;41:611–7.

Magnetic resonance imaging. Currently, MRI with delayed contrast enhancement (DCE) is the gold standard for non-invasive visualization of myocardial scar tissue. This technique is based on an inversion recovery pulse sequence and delayed imaging of the heart at approximately 10 – 20 minutes after administration of gadolinium-based contrast agents. Due to the chemical charge and molecular size of these gadolinium-based contrast agents, they rapidly diffuse from the intravascular to extracellular space, but do

not enter the intracellular space. Consequently, contrast accumulates within infarcted or scarred myocardial tissues. By selecting an appropriate inversion time to “null” normal myocardium, scar tissue will appear as bright hyperenhanced regions (Figure 15). The ability of MRI DCE to accurately depict scar tissue has been previously validated.¹⁰⁰ In the seminal paper by Kim et al., ex-vivo DCE images were displayed next to histopathological specimens of infarcted myocardial tissues, providing compelling evidence that the extent of delayed enhancement on MRI corresponded to histopathological infarct size.¹⁰⁰

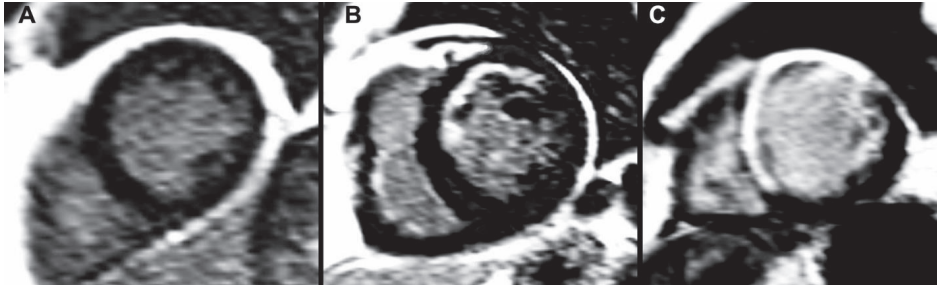


Figure 15. Examples of MRI delayed contrast-enhanced images. Panel A: normal study without evidence of delayed enhancement. Note that the normal myocardium appears black due to nulling by the inversion recovery pulse sequence. Panel B: non-transmural scarring in the anteroseptal and anterior segments appearing as white hyperenhanced regions indicative of previous subendocardial infarction in the left anterior descending artery territory. Panel C: transmural scarring in the septal, anteroseptal and anterior walls.

Kwong and co-workers demonstrated the prognostic value of identifying DCE in a cohort of 107 diabetic patients without previous clinical history of myocardial infarction.¹⁰¹ The presence of DCE, indicative of silent myocardial infarction, was associated with significantly higher all-cause mortality compared to diabetic patients without DCE (log rank $p = 0.02$). On multivariate analysis, the presence of DCE was the strongest independent predictor of major adverse cardiac outcomes (combination all-cause mortality, new acute myocardial infarction, hospitalization for unstable angina or heart failure, ventricular arrhythmias requiring implantable cardiac defibrillators, and acute cerebrovascular accidents) and all-cause mortality.

B) IMAGING LEFT VENTRICULAR MYOCARDIAL DYSFUNCTION IN DIABETIC HEART DISEASE

Although the etiology of diabetic heart disease is diverse and a source of on-going research, patients eventually develop evidence of increased myocardial fibrosis.¹⁰² These structural changes result in increased LV stiffness and impairment of diastolic and systolic performance. Although it is not a prerequisite for patients to have preexisting diabetic heart disease in order to develop heart failure, the presence of diabetic heart

disease increases the risk for subsequent development of heart failure. Thus, early detection of diabetic heart disease may permit early treatment and prevention of heart failure progression.

Currently, diagnosis of diabetic heart disease requires the demonstration of myocardial dysfunction that is independent of other causes such as significant coronary stenosis or hypertension. Thus, in diabetic patients with overt heart failure symptoms, the presence of echocardiographic features of LV dysfunction without other explanatory causes is often confirmatory for the diagnosis of diabetic cardiomyopathy. However, non-invasive imaging is usually required for the diagnosis of diabetic heart disease in patients without clinical signs and symptoms of heart failure. Often, echocardiography is utilized to demonstrate LV diastolic and systolic dysfunction in diabetic heart disease.

1. Diastolic function

Traditionally, LV diastolic function is categorized into normal, impaired relaxation, pseudonormal and restrictive filling patterns based on transmitral flow on echocardiography. These filling patterns occur sequentially with progressively worsening LV diastolic function. However, the interpretation of transmitral inflow pattern is severely hampered by its load- and age-dependency, and is also influenced by other factors such as atrial and ventricular compliance, mitral valve competency and left atrial pressures.¹⁰³

With the advent of tissue Doppler imaging, quantification of longitudinal myocardial velocities has significantly simplified the interpretation of LV diastolic function (Figure 16). Previous studies have demonstrated that the peak early diastolic e' velocity correlated significantly with the time constant of LV isovolumic relaxation (τ), the gold standard of LV diastolic function.^{104, 105} Transmitral inflow goes through a pseudonormalized pattern which can potentially be misinterpreted as normal, early diastolic e' velocity progressively declines with worsening LV diastolic function. However, tissue Doppler myocardial velocity imaging may be influenced by the passive translational motion and tethering effects from surrounding myocardial tissues. In contrast, myocardial strain and strain rate imaging permits site-specific quantification of active myocardial deformation that is independent of the translational motion and tethering artifacts.¹⁰⁶ Using strain rate imaging, LV diastolic function could be quantified by strain rate e' (Figures 17 and 18).¹⁰⁷ More recently, newer sophisticated echocardiographic techniques such as 2-dimensional speckle tracking have also been used to evaluate LV diastolic function (Figure 19).¹⁰⁸⁻¹¹⁰ Unlike tissue Doppler imaging, 2-dimensional speckle tracking is angle independent and may be more accurate than tissue Doppler imaging in evaluating LV diastolic function.^{108, 110}

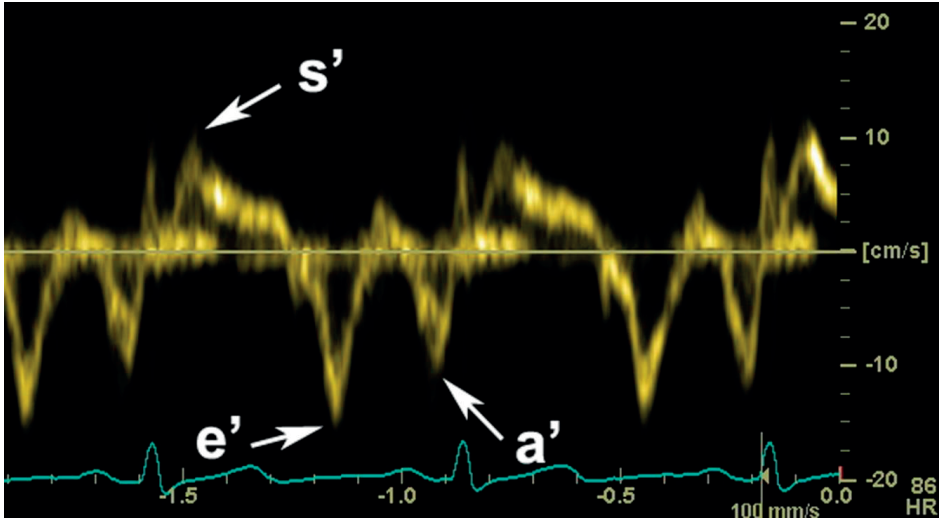


Figure 16. Example of pulsed wave tissue Doppler trace at the lateral mitral annulus. The cardiac cycle is presented by s' during systole, followed by early diastolic relaxation (e') and late diastolic atrial contraction (a') during diastole. LV systolic and diastolic function can be quantified by the peak s' (9.8 cm/s) and peak e' (15.2 cm/s) velocities respectively.

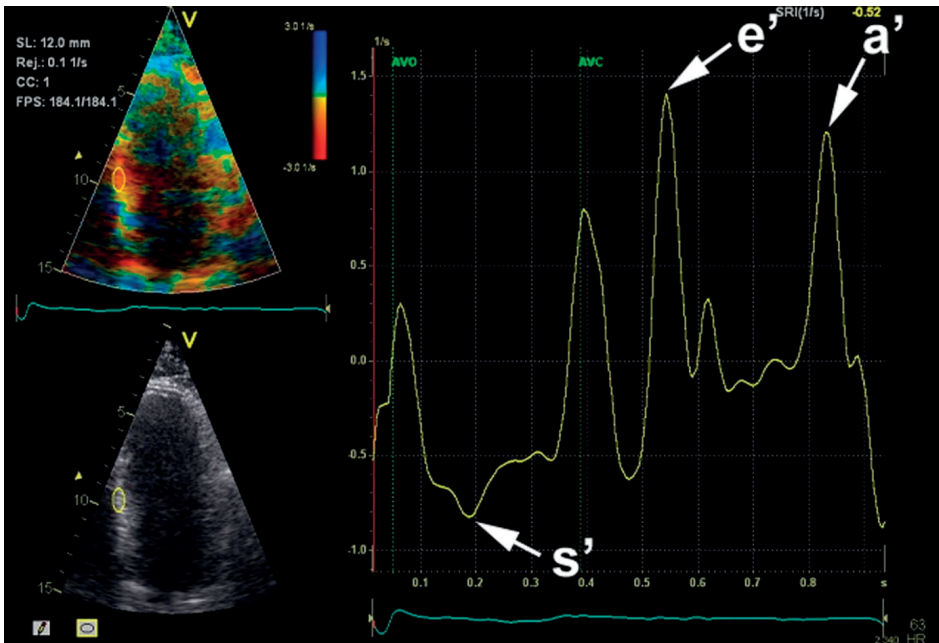


Figure 17. Example of strain rate tracing derived from color-coded tissue Doppler imaging of the mid septum. Similar to myocardial velocity imaging, myocardial strain rate can be divided into systolic (s'), early diastolic relaxation (e'), and late diastolic atrial (a') contractions. Myocardial systolic and diastolic function can be quantified by the peak s' (-0.84 s^{-1}) and e' (1.40 s^{-1}) strain rates respectively. AVO: aortic valve opening; AVC: aortic valve closure.

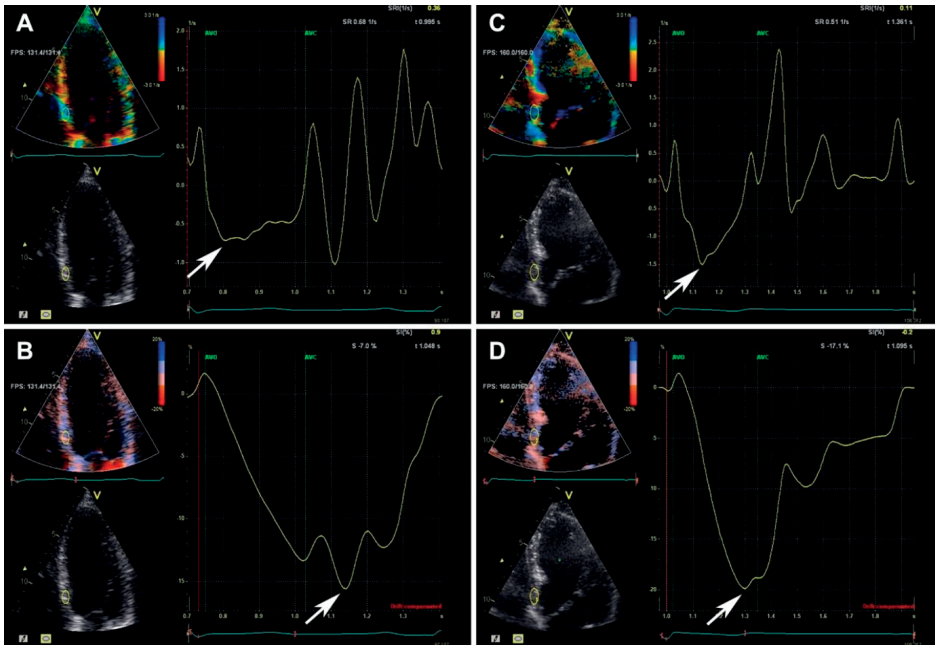


Figure 18. Examples of tissue Doppler derived strain rate and strain in a type 2 diabetic patient (Panels A and B respectively) and a normal healthy control (Panels C and D). Both the diabetic patient and normal control had comparable left ventricular ejection fraction (63% versus 66% respectively). However, the diabetic patient had significantly lower basal septal peak systolic strain rate and strain (-0.72 s^{-1} and -15.8% respectively, arrows) by tissue Doppler imaging compared to the normal healthy control (-1.50 s^{-1} and -19.9% respectively, arrows). AVO: aortic valve opening; AVC: aortic valve closure.

The most frequent finding in an asymptomatic patient with diabetic heart disease is diastolic dysfunction with normal LVEF. Even in well-controlled, normotensive and asymptomatic type 2 diabetic patients, the prevalence of diastolic dysfunction is reported to be up to 47% of patients, of which 30% had impaired relaxation and 17% had pseudo-normalized filling pattern.¹¹¹ However, newer and more sophisticated echocardiographic techniques such as tissue Doppler or 2-dimensional speckle tracking imaging are more sensitive in identifying subtle myocardial dysfunctions.^{109, 112-114} For example, using tissue Doppler imaging, Fang and co-workers determined that subclinical LV diastolic dysfunction was present in 21% of type 2 diabetic patients.¹¹⁴ This was in contrast to standard echocardiographic parameters such as transmitral inflow pattern, deceleration time and isovolumic relaxation time, which failed to identify subclinical diabetic heart disease. However, as the definition of significant subclinical LV dysfunction in that study was based on greater than 1 standard deviation less than the mean normal value derived from healthy controls, the true incidence of diabetic heart disease diagnosed with tissue Doppler imaging is likely to be significantly higher.¹¹⁴ Accordingly, Boyer and co-workers demonstrated that using a mitral annular velocity of $< 8 \text{ cm/s}$ identified up to 63% of diabetic patients as having evidence of diastolic dysfunction.¹¹²

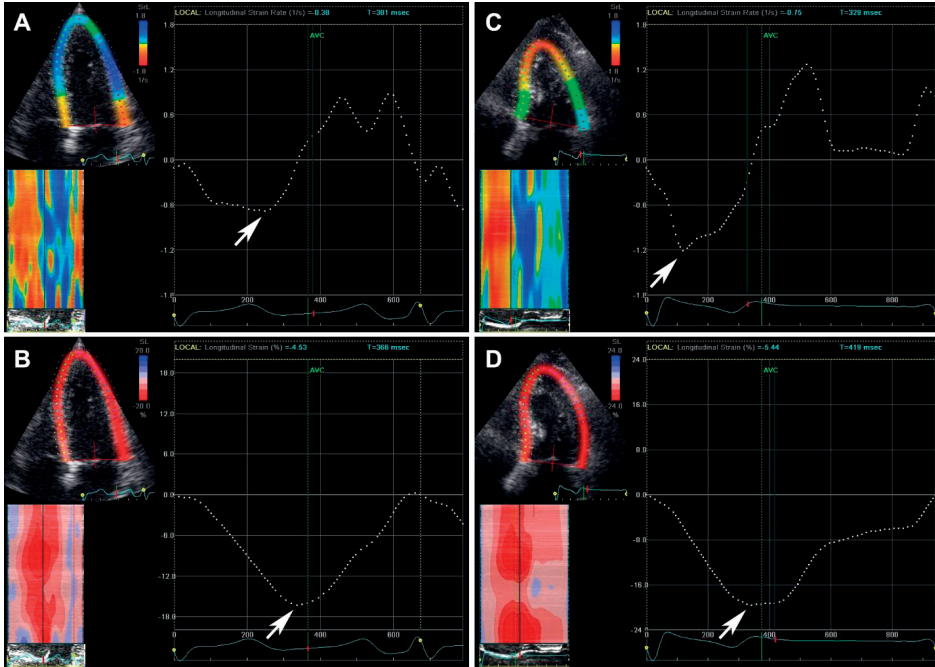


Figure 19. Examples of 2-dimensional speckle tracking strain and strain rate in the same diabetic patient and normal control. The diabetic patient had significantly lower peak global systolic strain rate and strain (-0.69 s^{-1} and -16.3% respectively, arrows) by 2-dimensional speckle tracking compared to the normal control (-1.22 s^{-1} and -20.1% respectively, arrows). AVC: aortic valve closure.

2. Systolic function

Traditionally, the clinical standard in the assessment of global LV systolic function is primarily based on the quantification of LV chamber volumes to derive LVEF. Although quantification of systolic function by LVEF is easily understandable and reasonably reproducible, it is highly dependent in preload and afterload. Due to the relative insensitivity of LVEF in detecting subtle myocardial dysfunction, demonstrating LV systolic dysfunction in diabetic patients has been more difficult. In contrast, myocardial velocity, strain and strain rate imaging are more sensitive systolic markers than LVEF. Similarly, quantification of systolic function by myocardial velocity (Figure 16), strain and strain rate imaging (Figures 17-19) has been shown to be significantly correlated with global LV systolic function.^{106, 115-117}

Previous studies have demonstrated subclinical myocardial systolic dysfunction in diabetic patients.^{97, 109, 113, 118, 119} Using color-coded tissue Doppler imaging, Fang and co-workers demonstrated reduced myocardial longitudinal systolic function in diabetic patients compared to age-matched controls.¹¹³ In that study, diabetic patients had significantly lower peak systolic strain rate compared to controls ($1.4 \pm 0.3 \text{ s}^{-1}$ vs. 1.6 ± 0.3

s^{-1} , $p = 0.006$), suggesting the presence of subtle myocardial contractile dysfunction despite normal LVEF. Similarly, Galderisi and co-workers examined the value of myocardial systolic velocity and strain rate during dobutamine stress echocardiography in 24 diabetic patients and 16 normal controls.¹¹⁹ The group demonstrated that diabetic patients had evidence of reduced myocardial contractile reserve compared to non-diabetics. Therefore, tissue Doppler imaging is more sensitive than conventional LVEF in detecting subclinical myocardial systolic dysfunction. More recently, Ng and co-workers utilized 2-dimensional speckle tracking echocardiography to compare type 2 diabetic patients with normal healthy controls.¹⁰⁹ Despite all the diabetic patients having good glycemic control and asymptomatic without evidence of diabetic complications, coronary artery disease and hypertension, 2-dimensional speckle tracking was able to identify significant subclinical LV dysfunction compared to the controls.¹⁰⁹ Diabetic patients had significantly lower global longitudinal strain ($-18.3 \pm 2.2\%$ vs. $-19.9 \pm 1.9\%$, $p < 0.001$) and systolic strain rate ($-0.99 \pm 0.17 s^{-1}$ vs. $-1.07 \pm 0.13 s^{-1}$, $p = 0.009$) compared to healthy controls.¹⁰⁹

3. Regional differences in myocardial dysfunction in diabetic heart disease

The LV myocardial architecture is a complex array of longitudinally and circumferentially orientated fibres located predominately in the epicardium/endocardium and mid-wall respectively.¹²⁰ Newer and more sophisticated echocardiographic techniques allow site-specific and multidirectional assessments of myocardial strain and strain rate, thereby permitting exploration of regional differences in myocardial functional changes in subclinical diabetic heart disease. Using color-coded tissue Doppler imaging, both Fang et al. and Vinereanu et al. demonstrated reduced longitudinal myocardial function with a compensatory increase in radial function.^{113, 118} Similarly, using multidirectional speckle tracking analyses, Ng and co-workers demonstrated reduced longitudinal strain and strain rate (predominantly derived from epicardial/endocardial fibre contraction) but preserved circumferential and radial strains and strain rates (predominantly derived from mid-wall circumferential fibres contraction) in asymptomatic diabetic patients.¹⁰⁹ These findings suggest that myocardial dysfunction in early diabetic cardiomyopathy may start in the subendocardium, and the preservation of circumferential and radial functions account for the initial preservation of LV volumes and EF.

C) CONCLUSIONS

Over the last few decades, there is increasing recognition that diabetic heart disease is a real disease entity rather than a nebulous concept, supported by evidence from epi-

demioleological and experimental studies that demonstrated an independent association between diabetes and heart failure. Numerous studies have explored the underlying pathophysiological mechanisms triggering the disease onset and progression to overt clinical heart failure. However, the etiology of diabetic heart disease remains unclear and is likely to be multifactorial, such as altered myocardial metabolism, endothelial dysfunction, autonomic neuropathy, coronary atherosclerosis and increased myocardial fibrosis. Multimodality imaging including echocardiography, nuclear imaging, CT and MRI all provide valuable insights into the disease process. In addition, cardiac imaging is essential for diagnosing diabetic heart disease by demonstrating LV myocardial dysfunction that is independent of significant coronary artery disease and hypertension. Finally, multimodality cardiac imaging may be useful for monitoring disease progression and evaluate the effectiveness of medical interventions.

REFERENCE LIST

- (1) World Health Organization. Definition and diagnosis of diabetes mellitus and intermediate hyperglycemia. 2006.
- (2) Wild S, Roglic G, Green A, Sicree R, King H. Global Prevalence of Diabetes. *Diabetes Care* 2004;27:1047-1053.
- (3) Kannel WB, McGee DL. Diabetes and cardiovascular disease. The Framingham study. *JAMA* 1979;241:2035-2038.
- (4) From AM, Scott CG, Chen HH. The Development of Heart Failure in Patients With Diabetes Mellitus and Pre-Clinical Diastolic Dysfunction: A Population-Based Study. *J Am Coll Cardiol* 2010;55:300-305.
- (5) Coughlin SS, Pearle DL, Baughman KL, Wasserman A, Tefft MC. Diabetes mellitus and risk of idiopathic dilated cardiomyopathy. The Washington, DC Dilated Cardiomyopathy Study. *Ann Epidemiol* 1994;4:67-74.
- (6) Redfield MM, Jacobsen SJ, Burnett JC, Jr., Mahoney DW, Bailey KR, Rodeheffer RJ. Burden of systolic and diastolic ventricular dysfunction in the community: appreciating the scope of the heart failure epidemic. *JAMA* 2003;289:194-202.
- (7) Nichols GA, Gullion CM, Koro CE, Ephross SA, Brown JB. The incidence of congestive heart failure in type 2 diabetes: an update. *Diabetes Care* 2004;27:1879-1884.
- (8) Rubler S, Dlugash J, Yuceoglu YZ, Kumral T, Branwood AW, Grishman A. New type of cardiomyopathy associated with diabetic glomerulosclerosis. *Am J Cardiol* 1972;30:595-602.
- (9) Boudina S, Abel ED. Diabetic Cardiomyopathy Revisited. *Circulation* 2007;115:3213-3223.
- (10) Marwick T. The diabetic myocardium. *Curr Diab Rep* 2006;6:36-41.
- (11) Lindsey JB, Marso SP. Steatosis and Diastolic Dysfunction: The Skinny on Myocardial Fat. *J Am Coll Cardiol* 2008;52:1800-1802.
- (12) Schaffer JE. Lipotoxicity: when tissues overeat. *Curr Opin Lipidol* 2003;14:281-287.
- (13) McGavock JM, Victor RG, Unger RH, Szczepaniak LS. Adiposity of the Heart, Revisited. *Ann Intern Med* 2006;144:517-524.
- (14) Lopaschuk GD, Ussher JR, Folmes CD, Jaswal JS, Stanley WC. Myocardial fatty acid metabolism in health and disease. *Physiol Rev* 2010;90:207-258.
- (15) Unger RH. Lipotoxic Diseases. *Annu Rev Med* 2002;53:319.
- (16) Szczepaniak LS, Dobbins RL, Metzger GJ, Sartoni-D'Ambrosia G, Arbique D, Vongpatanasin W, Unger R, Victor RG. Myocardial triglycerides and systolic function in humans: in vivo evaluation by localized proton spectroscopy and cardiac imaging. *Magn Reson Med* 2003;49:417-423.
- (17) van der Meer RW, Doornbos J, Kozerke S, Schar M, Bax JJ, Hammer S, Smit JW, Romijn JA, Diamant M, Rijzewijk LJ, De Roos A, Lamb HJ. Metabolic imaging of myocardial triglyceride content: reproducibility of 1H MR spectroscopy with respiratory navigator gating in volunteers. *Radiology* 2007;245:251-257.
- (18) Hammer S, Snel M, Lamb HJ, Jazet IM, van der Meer RW, Pijl H, Meinders EA, Romijn JA, De Roos A, Smit JW. Prolonged caloric restriction in obese patients with type 2 diabetes mellitus decreases myocardial triglyceride content and improves myocardial function. *J Am Coll Cardiol* 2008;52:1006-1012.

- (19) Iozzo P, Lautamaki R, Borra R, Lehto HR, Bucci M, Viljanen A, Parkka J, Lepomaki V, Maggio R, Parkkola R, Nuuti J, Nuutila P. Contribution of glucose tolerance and gender to cardiac adiposity. *J Clin Endocrinol Metab* 2009;94:4472-4482.
- (20) Rijzewijk LJ, van der Meer RW, Smit JWA, Diamant M, Bax JJ, Hammer S, Romijn JA, De Roos A, Lamb HJ. Myocardial Steatosis Is an Independent Predictor of Diastolic Dysfunction in Type 2 Diabetes Mellitus. *J Am Coll Cardiol* 2008;52:1793-1799.
- (21) van der Meer RW, Rijzewijk LJ, Diamant M, Hammer S, Schar M, Bax JJ, Smit JW, Romijn JA, De Roos A, Lamb HJ. The ageing male heart: myocardial triglyceride content as independent predictor of diastolic function. *Eur Heart J* 2008;29:1516-1522.
- (22) van der Meer RW, Rijzewijk LJ, de Jong HWAM, Lamb HJ, Lubberink M, Romijn JA, Bax JJ, De Roos A, Kamp O, Paulus WJ, Heine RJ, Lammertsma AA, Smit JWA, Diamant M. Pioglitazone Improves Cardiac Function and Alters Myocardial Substrate Metabolism Without Affecting Cardiac Triglyceride Accumulation and High-Energy Phosphate Metabolism in Patients With Well-Controlled Type 2 Diabetes Mellitus. *Circulation* 2009;119:2069-2077.
- (23) McGavock JM, Lingvay I, Zib I, Tillery T, Salas N, Unger R, Levine BD, Raskin P, Victor RG, Szczepaniak LS. Cardiac Steatosis in Diabetes Mellitus: A 1H-Magnetic Resonance Spectroscopy Study. *Circulation* 2007;116:1170-1175.
- (24) Sharma S, Adroque JV, Golfman L, Uray I, Lemm J, Youker K, Noon GP, Frazier OH, Taegtmeier H. Intramyocardial lipid accumulation in the failing human heart resembles the lipotoxic rat heart. *FASEB J* 2004;18:1692-1700.
- (25) Zhou YT, Grayburn P, Karim A, Shimabukuro M, Higa M, Baetens D, Orci L, Unger RH. Lipotoxic heart disease in obese rats: Implications for human obesity. *Proc Natl Acad Science USA* 2000;97:1784-1789.
- (26) Schrauwen-Hinderling VB, Hesselink MK, Meex R, van der MS, Schar M, Lamb H, Wildberger JE, Glatz J, Snoep G, Kooi ME, Schrauwen P. Improved Ejection Fraction after Exercise Training in Obesity Is Accompanied by Reduced Cardiac Lipid Content. *J Clin Endocrinol Metab* 2010;95:1932-1938.
- (27) Zib I, Jacob AN, Lingvay I, Salinas K, McGavock JM, Raskin P, Szczepaniak LS. Effect of pioglitazone therapy on myocardial and hepatic steatosis in insulin-treated patients with type 2 diabetes. *J Investig Med* 2007;55:230-236.
- (28) Kinlay S, Libby P, Ganz P. Endothelial function and coronary artery disease. *Curr Opin Lipidol* 2001;12:383-389.
- (29) Radomski MW, Palmer RM, Moncada S. The role of nitric oxide and cGMP in platelet adhesion to vascular endothelium. *Biochem Biophys Res Commun* 1987;148:1482-1489.
- (30) Kubes P, Suzuki M, Granger DN. Nitric oxide: an endogenous modulator of leukocyte adhesion. *Proc Natl Acad Sci U S A* 1991;88:4651-4655.
- (31) Sarkar R, Meinberg EG, Stanley JC, Gordon D, Webb RC. Nitric oxide reversibly inhibits the migration of cultured vascular smooth muscle cells. *Circ Res* 1996;78:225-230.
- (32) Creager MA, Luscher TF, Cosentino F, Beckman JA. Diabetes and vascular disease: pathophysiology, clinical consequences, and medical therapy: Part I. *Circulation* 2003;108:1527-1532.
- (33) Tan KC, Chow WS, Ai VH, Metz C, Bucala R, Lam KS. Advanced glycation end products and endothelial dysfunction in type 2 diabetes. *Diabetes Care* 2002;25:1055-1059.

- (34) McDaid EA, Monaghan B, Parker AI, Hayes JR, Allen JA. Peripheral autonomic impairment in patients newly diagnosed with type II diabetes. *Diabetes Care* 1994;17:1422-1427.
- (35) Celermajer DS, Sorensen KE, Gooch VM, Spiegelhalter DJ, Miller OI, Sullivan ID, Lloyd JK, Deanfield JE. Non-invasive detection of endothelial dysfunction in children and adults at risk of atherosclerosis. *Lancet* 1992;340:1111-1115.
- (36) Anderson TJ, Uehata A, Gerhard MD, Meredith IT, Knab S, Delagrange D, Lieberman EH, Ganz P, Creager MA, Yeung AC. Close relation of endothelial function in the human coronary and peripheral circulations. *J Am Coll Cardiol* 1995;26:1235-1241.
- (37) Deanfield JE, Halcox JP, Rabelink TJ. Endothelial function and dysfunction: testing and clinical relevance. *Circulation* 2007;115:1285-1295.
- (38) Bots ML, Westerink J, Rabelink TJ, de Koning EJ. Assessment of flow-mediated vasodilatation (FMD) of the brachial artery: effects of technical aspects of the FMD measurement on the FMD response. *Eur Heart J* 2005;26:363-368.
- (39) Kang X, Berman DS, Lewin H, Miranda R, Erel J, Friedman JD, Amanullah AM. Comparative ability of myocardial perfusion single-photon emission computed tomography to detect coronary artery disease in patients with and without diabetes mellitus. *Am Heart J* 1999;137:949-957.
- (40) Djaberi R, Roodt J, Schuijff JD, Rabelink TJ, de Koning EJ, Pereira AM, Stokkel MP, Smit JW, Bax JJ, Jukema JW. Endothelial dysfunction in diabetic patients with abnormal myocardial perfusion in the absence of epicardial obstructive coronary artery disease. *J Nucl Med* 2009;50:1980-1986.
- (41) Fang ZY, Najos-Valencia O, Leano R, Marwick TH. Patients with early diabetic heart disease demonstrate a normal myocardial response to dobutamine. *J Am Coll Cardiol* 2003;42:446-453.
- (42) Moir S, Hanekom L, Fang ZY, Haluska B, Wong C, Burgess M, Marwick TH. Relationship between myocardial perfusion and dysfunction in diabetic cardiomyopathy: a study of quantitative contrast echocardiography and strain rate imaging. *Heart* 2006;92:1414-1419.
- (43) Wei K, Ragosta M, Thorpe J, Coggins M, Moos S, Kaul S. Noninvasive quantification of coronary blood flow reserve in humans using myocardial contrast echocardiography. *Circulation* 2001;103:2560-2565.
- (44) Hansen CL, Goldstein RA, Akinboboye OO, Berman DS, Botvinick EH, Churchwell KB, Cooke CD, Corbett JR, Cullom SJ, Dahlberg ST, Druz RS, Ficaro EP, Galt JR, Garg RK, Germano G, Heller GV, Henzlava MJ, Hyun MC, Johnson LL, Mann A, McCallister BD, Jr., Quaife RA, Ruddy TD, Sundaram SN, Taillefer R, Ward RP, Mahmarian JJ. Myocardial perfusion and function: single photon emission computed tomography. *J Nucl Cardiol* 2007;14:e39-e60.
- (45) Amanullah AM, Berman DS, Hachamovitch R, Kiat H, Kang X, Friedman JD. Identification of severe or extensive coronary artery disease in women by adenosine technetium-99m sestamibi SPECT. *Am J Cardiol* 1997;80:132-137.
- (46) Hasdai D, Gibbons RJ, Holmes DR, Jr., Higano ST, Lerman A. Coronary endothelial dysfunction in humans is associated with myocardial perfusion defects. *Circulation* 1997;96:3390-3395.
- (47) Wackers FJ, Young LH, Inzucchi SE, Chyun DA, Davey JA, Barrett EJ, Taillefer R, Wittlin SD, Heller GV, Filipchuk N, Engel S, Ratner RE, Iskandrian AE. Detection of silent myocardial ischemia in asymptomatic diabetic subjects: the DIAD study. *Diabetes Care* 2004;27:1954-1961.
- (48) Valensi P, Paries J, Brulport-Cerisier V, Torremocha F, Sachs RN, Vanzetto G, Cosson E, Lormeau B, Attali JR, Marechaud R, Estour B, Halimi S. Predictive value of silent myocardial ischemia for

- cardiac events in diabetic patients: influence of age in a French multicenter study. *Diabetes Care* 2005;28:2722-2727.
- (49) Zellweger MJ, Hachamovitch R, Kang X, Hayes SW, Friedman JD, Germano G, Pfisterer ME, Berman DS. Prognostic relevance of symptoms versus objective evidence of coronary artery disease in diabetic patients. *Eur Heart J* 2004;25:543-550.
- (50) Kang X, Berman DS, Lewin HC, Cohen I, Friedman JD, Germano G, Hachamovitch R, Shaw LJ. Incremental prognostic value of myocardial perfusion single photon emission computed tomography in patients with diabetes mellitus. *Am Heart J* 1999;138:1025-1032.
- (51) Pancholy SB, Fattah AA, Kamal AM, Ghods M, Heo J, Iskandrian AS. Independent and incremental prognostic value of exercise thallium single-photon emission computed tomographic imaging in women. *J Nucl Cardiol* 1995;2:110-116.
- (52) Ross R. The pathogenesis of atherosclerosis: a perspective for the 1990s. *Nature* 1993;362:801-809.
- (53) Egashira K, Hirooka Y, Kai H, Sugimachi M, Suzuki S, Inou T, Takeshita A. Reduction in serum cholesterol with pravastatin improves endothelium-dependent coronary vasomotion in patients with hypercholesterolemia. *Circulation* 1994;89:2519-2524.
- (54) Wackers FJ, Chyun DA, Young LH, Heller GV, Iskandrian AE, Davey JA, Barrett EJ, Taillefer R, Wittlin SD, Filipchuk N, Ratner RE, Inzucchi SE. Resolution of asymptomatic myocardial ischemia in patients with type 2 diabetes in the Detection of Ischemia in Asymptomatic Diabetics (DIAD) study. *Diabetes Care* 2007;30:2892-2898.
- (55) Bateman TM, Heller GV, McGhie AI, Friedman JD, Case JA, Bryngelson JR, Hertenstein GK, Moutray KL, Reid K, Cullom SJ. Diagnostic accuracy of rest/stress ECG-gated Rb-82 myocardial perfusion PET: comparison with ECG-gated Tc-99m sestamibi SPECT. *J Nucl Cardiol* 2006;13:24-33.
- (56) Bengel FM, Higuchi T, Javadi MS, Lautamaki R. Cardiac positron emission tomography. *J Am Coll Cardiol* 2009;54:1-15.
- (57) Bergmann SR, Herrero P, Markham J, Weinheimer CJ, Walsh MN. Noninvasive quantitation of myocardial blood flow in human subjects with oxygen-15-labeled water and positron emission tomography. *J Am Coll Cardiol* 1989;14:639-652.
- (58) Lortie M, Beanlands RS, Yoshinaga K, Klein R, Dasilva JN, DeKemp RA. Quantification of myocardial blood flow with 82Rb dynamic PET imaging. *Eur J Nucl Med Mol Imaging* 2007;34:1765-1774.
- (59) Kaufmann PA, Gnechi-Ruscione T, Yap JT, Rimoldi O, Camici PG. Assessment of the reproducibility of baseline and hyperemic myocardial blood flow measurements with 15O-labeled water and PET. *J Nucl Med* 1999;40:1848-1856.
- (60) Campisi R, Czernin J, Schoder H, Sayre JW, Marengo FD, Phelps ME, Schelbert HR. Effects of long-term smoking on myocardial blood flow, coronary vasomotion, and vasodilator capacity. *Circulation* 1998;98:119-125.
- (61) Pitkanen OP, Raitakari OT, Niinikoski H, Nuutila P, Iida H, Voipio-Pulkki LM, Harkonen R, Wegelius U, Ronnema T, Viikari J, Knuuti J. Coronary flow reserve is impaired in young men with familial hypercholesterolemia. *J Am Coll Cardiol* 1996;28:1705-1711.
- (62) Kjaer A, Meyer C, Nielsen FS, Parving HH, Hesse B. Dipyridamole, cold pressor test, and demonstration of endothelial dysfunction: a PET study of myocardial perfusion in diabetes. *J Nucl Med* 2003;44:19-23.

- (63) Momose M, Abletshauser C, Neerve J, Nekolla SG, Schnell O, Standl E, Schwaiger M, Bengel FM. Dysregulation of coronary microvascular reactivity in asymptomatic patients with type 2 diabetes mellitus. *Eur J Nucl Med Mol Imaging* 2002;29:1675-1679.
- (64) Prior JO, Quinones MJ, Hernandez-Pampaloni M, Facta AD, Schindler TH, Sayre JW, Hsueh WA, Schelbert HR. Coronary circulatory dysfunction in insulin resistance, impaired glucose tolerance, and type 2 diabetes mellitus. *Circulation* 2005;111:2291-2298.
- (65) Taskiran M, Fritz-Hansen T, Rasmussen V, Larsson HB, Hilsted J. Decreased myocardial perfusion reserve in diabetic autonomic neuropathy. *Diabetes* 2002;51:3306-3310.
- (66) Vinik AI, Freeman R, Erbas T. Diabetic autonomic neuropathy. *Semin Neurol* 2003;23:365-372.
- (67) Boulton AJ, Vinik AI, Arezzo JC, Bril V, Feldman EL, Freeman R, Malik RA, Maser RE, Sosenko JM, Ziegler D. Diabetic neuropathies: a statement by the American Diabetes Association. *Diabetes Care* 2005;28:956-962.
- (68) Nagamachi S, Fujita S, Nishii R, Futami S, Tamura S, Mizuta M, Nakazato M, Kurose T, Wakamatsu H. Prognostic value of cardiac I-123 metaiodobenzylguanidine imaging in patients with non-insulin-dependent diabetes mellitus. *J Nucl Cardiol* 2006;13:34-42.
- (69) Vinik AI, Ziegler D. Diabetic cardiovascular autonomic neuropathy. *Circulation* 2007;115:387-397.
- (70) Vinik AI, Maser RE, Mitchell BD, Freeman R. Diabetic autonomic neuropathy. *Diabetes Care* 2003;26:1553-1579.
- (71) Vinik AI, Ziegler D. Diabetic cardiovascular autonomic neuropathy. *Circulation* 2007;115:387-397.
- (72) Vinik AI, Ziegler D. Diabetic cardiovascular autonomic neuropathy. *Circulation* 2007;115:387-397.
- (73) Vinik AI, Ziegler D. Diabetic cardiovascular autonomic neuropathy. *Circulation* 2007;115:387-397.
- (74) Ziegler D, Weise F, Langen KJ, Piolot R, Boy C, Hubinger A, Muller-Gartner HW, Gries FA. Effect of glycaemic control on myocardial sympathetic innervation assessed by [123I]metaiodobenzylguanidine scintigraphy: a 4-year prospective study in IDDM patients. *Diabetologia* 1998;41:443-451.
- (75) Stevens MJ, Raffel DM, Allman KC, Dayanikli F, Ficaro E, Sandford T, Wieland DM, Pfeifer MA, Schwaiger M. Cardiac sympathetic dysinnervation in diabetes: implications for enhanced cardiovascular risk. *Circulation* 1998;98:961-968.
- (76) Patel AD, Iskandrian AE. MIBG imaging. *J Nucl Cardiol* 2002;9:75-94.
- (77) Allman KC, Stevens MJ, Wieland DM, Hutchins GD, Wolfe ER, Jr., Greene DA, Schwaiger M. Noninvasive assessment of cardiac diabetic neuropathy by carbon-11 hydroxyephedrine and positron emission tomography. *J Am Coll Cardiol* 1993;22:1425-1432.
- (78) Nagamachi S, Jinnouchi S, Kurose T, Nishii R, Kawai K, Futami S, Tamura S, Matsukura S. Serial change in 123I-MIBG myocardial scintigraphy in non-insulin-dependent diabetes mellitus. *Ann Nucl Med* 2002;16:33-38.
- (79) Verberne HJ, Brewster LM, Somsen GA, Eck-Smit BL. Prognostic value of myocardial 123I-metaiodobenzylguanidine (MIBG) parameters in patients with heart failure: a systematic review. *Eur Heart J* 2008;29:1147-1159.
- (80) Turpeinen AK, Vanninen E, Kuikka JT, Uusitupa MI. Demonstration of regional sympathetic denervation of the heart in diabetes. Comparison between patients with NIDDM and IDDM. *Diabetes Care* 1996;19:1083-1090.

- (81) Goraya TY, Leibson CL, Palumbo PJ, Weston SA, Killian JM, Pfeifer EA, Jacobsen SJ, Frye RL, Roger VL. Coronary atherosclerosis in diabetes mellitus: a population-based autopsy study. *J Am Coll Cardiol* 2002;40:946-953.
- (82) Pundziute G, Schuijff JD, Jukema JW, Boersma E, de RA, van der Wall EE, Bax JJ. Prognostic value of multislice computed tomography coronary angiography in patients with known or suspected coronary artery disease. *J Am Coll Cardiol* 2007;49:62-70.
- (83) Ambrose JA, Tannenbaum MA, Alexopoulos D, Hjemdahl-Monsen CE, Leavy J, Weiss M, Borrico S, Gorlin R, Fuster V. Angiographic progression of coronary artery disease and the development of myocardial infarction. *J Am Coll Cardiol* 1988;12:56-62.
- (84) Little WC, Constantinescu M, Applegate RJ, Kutcher MA, Burrows MT, Kahl FR, Santamore WP. Can coronary angiography predict the site of a subsequent myocardial infarction in patients with mild-to-moderate coronary artery disease? *Circulation* 1988;78:1157-1166.
- (85) Sarwar A, Shaw LJ, Shapiro MD, Blankstein R, Hoffman U, Cury RC, Abbara S, Brady TJ, Budoff MJ, Blumenthal RS, Nasir K. Diagnostic and prognostic value of absence of coronary artery calcification. *J Am Coll Cardiol Img* 2009;2:675-688.
- (86) Budoff MJ, Shaw LJ, Liu ST, Weinstein SR, Mosler TP, Tseng PH, Flores FR, Callister TQ, Raggi P, Berman DS. Long-term prognosis associated with coronary calcification: observations from a registry of 25,253 patients. *J Am Coll Cardiol* 2007;49:1860-1870.
- (87) Raggi P, Shaw LJ, Berman DS, Callister TQ. Prognostic value of coronary artery calcium screening in subjects with and without diabetes. *J Am Coll Cardiol* 2004;43:1663-1669.
- (88) Anand DV, Lim E, Hopkins D, Corder R, Shaw LJ, Sharp P, Lipkin D, Lahiri A. Risk stratification in uncomplicated type 2 diabetes: prospective evaluation of the combined use of coronary artery calcium imaging and selective myocardial perfusion scintigraphy. *Eur Heart J* 2006;27:713-721.
- (89) Burgstahler C, Beck T, Reimann A, Kuettner A, Kopp AF, Heuschmid M, Claussen CD, Schroeder S. Diagnostic accuracy of multislice computed tomography for the detection of coronary artery disease in diabetic patients. *J Diabetes Complications* 2007;21:69-74.
- (90) Schuijff JD, Bax JJ, Jukema JW, Lamb HJ, Vliegen HW, Salm LP, De Roos A, Van Der Wall E. Non-invasive angiography and assessment of left ventricular function using multislice computed tomography in patients with type 2 diabetes. *Diabetes Care* 2004;27:2905-2910.
- (91) Pundziute G, Schuijff JD, Jukema JW, Boersma E, Scholte AJ, Kroft LJ, van der Wall EE, Bax JJ. Noninvasive assessment of plaque characteristics with multislice computed tomography coronary angiography in symptomatic diabetic patients. *Diabetes Care* 2007;30:1113-1119.
- (92) Pundziute G, Schuijff JD, Jukema JW, van Werkhoven JM, Nucifora G, Decramer I, Sarno G, Vanhoenacker PK, Reiber JH, Wijns W, Bax JJ. Type 2 diabetes is associated with more advanced coronary atherosclerosis on multislice computed tomography and virtual histology intravascular ultrasound. *J Nucl Cardiol* 2009;16:376-383.
- (93) Scholte AJ, Schuijff JD, Kharagjitsingh AV, Jukema JW, Pundziute G, van der Wall EE, Bax JJ. Prevalence of coronary artery disease and plaque morphology assessed by multi-slice computed tomography coronary angiography and calcium scoring in asymptomatic patients with type 2 diabetes. *Heart* 2008;94:290-295.
- (94) van Werkhoven JM, Cademartiri F, Seitun S, Maffei E, Palumbo A, Martini C, Tarantini G, Kroft LJ, De Roos A, Weustink AC, Jukema JW, Ardissino D, Mollet NR, Schuijff JD, Bax JJ. Prognostic Value

- of Computed Tomographic Coronary Angiography in Patients with Diabetes: Comparison with a Non-diabetic Population. *Radiology*. In press 2010.
- (95) Kawaguchi M, Techigawara M, Ishihata T, Asakura T, Saito F, Maehara K, Maruyama Y. A comparison of ultrastructural changes on endomyocardial biopsy specimens obtained from patients with diabetes mellitus with and without hypertension. *Heart Vessels* 1997;12:267-274.
 - (96) Adeghate E. Molecular and cellular basis of the aetiology and management of diabetic cardiomyopathy: a short review. *Mol Cell Biochem* 2004;261:187-191.
 - (97) Loganathan R, Bilgen M, Al Hafez B, Smirnova IV. Characterization of alterations in diabetic myocardial tissue using high resolution MRI. *Int J Cardiovasc Imaging* 2006;22:81-90.
 - (98) Picano E, Pelosi G, Marzilli M, Lattanzi F, Benassi A, Landini L, L'Abbate A. In vivo quantitative ultrasonic evaluation of myocardial fibrosis in humans. *Circulation* 1990;81:58-64.
 - (99) Di B, V, Talarico L, Picano E, Di MC, Landini L, Paterni M, Matteucci E, Giusti C, Giampietro O. Increased echodensity of myocardial wall in the diabetic heart: an ultrasound tissue characterization study. *J Am Coll Cardiol* 1995;25:1408-1415.
 - (100) Fang ZY, Yuda S, Anderson V, Short L, Case C, Marwick TH. Echocardiographic detection of early diabetic myocardial disease. *J Am Coll Cardiol* 2003;41:611-617.
 - (101) Regan TJ, Wu CF, Yeh CK, Oldewurtel HA, Haider B. Myocardial composition and function in diabetes. The effects of chronic insulin use. *Circ Res* 1981;49:1268-1277.
 - (102) Bhimji S, Godin DV, McNeill JH. Biochemical and functional changes in hearts from rabbits with diabetes. *Diabetologia* 1985;28:452-457.
 - (103) Kim RJ, Fieno DS, Parrish TB, Harris K, Chen EL, Simonetti O, Bundy J, Finn JP, Klocke FJ, Judd RM. Relationship of MRI delayed contrast enhancement to irreversible injury, infarct age, and contractile function. *Circulation* 1999;100:1992-2002.
 - (104) Kwong RY, Sattar H, Wu H, Vorobiof G, Gandla V, Steel K, Siu S, Brown KA. Incidence and prognostic implication of unrecognized myocardial scar characterized by cardiac magnetic resonance in diabetic patients without clinical evidence of myocardial infarction. *Circulation* 2008;118:1011-1020.
 - (105) Aneja A, Tang WH, Bansilal S, Garcia MJ, Farkouh ME. Diabetic cardiomyopathy: insights into pathogenesis, diagnostic challenges, and therapeutic options. *Am J Med* 2008;121:748-757.
 - (106) Nagueh SF, Appleton CP, Gillebert TC, Marino PN, Oh JK, Smiseth OA, Waggoner AD, Flachskampf FA, Pellikka PA, Evangelista A. Recommendations for the evaluation of left ventricular diastolic function by echocardiography. *J Am Soc Echocardiogr* 2009;22:107-133.
 - (107) Nagueh SF., Middleton KJ., Kopelen HA., Zoghbi WA., Quinones MA. Doppler Tissue Imaging: A Noninvasive Technique for Evaluation of Left Ventricular Relaxation and Estimation of Filling Pressures. *J Am Coll Cardiol* 1997;30:1527-1533.
 - (108) Nagueh SF, Sun H, Kopelen HA, Middleton KJ, Khoury DS. Hemodynamic determinants of the mitral annulus diastolic velocities by tissue Doppler. *J Am Coll Cardiol* 2001;37:278-285.
 - (109) Leung DY, Ng AC. Emerging clinical role of strain imaging in echocardiography. *Heart Lung Circ* 2010;19:161-174.
 - (110) Marwick TH. Measurement of Strain and Strain Rate by Echocardiography: Ready for Prime Time? *J Am Coll Cardiol* 2006;47:1313-1327.

- (111) Ng ACT, Tran DT, Newman M, Allman C, Vidaic J, Kadappu KK, Boyd A, Thomas L, Leung DY. Comparison of Myocardial Tissue Velocities Measured by Two-Dimensional Speckle Tracking and Tissue Doppler Imaging. *Am J Cardiol* 2008;102:784-789.
- (112) Ng ACT, Delgado V, Bertini M, van der Meer RW, Rijzewijk LJ, Shanks M, Nucifora G, Smit JWA, Diamant M, Romijn JA, De Roos A, Leung DY, Lamb HJ, Bax JJ. Findings from left ventricular strain and strain rate imaging in asymptomatic patients with type 2 diabetes mellitus. *Am J Cardiol* 2009;104:1398-1401.
- (113) van Dalen BM, Bosch JG, Kauer F, Soliman OI, Vletter WB, ten Cate FJ, Geleijnse ML. Assessment of mitral annular velocities by speckle tracking echocardiography versus tissue Doppler imaging: validation, feasibility, and reproducibility. *J Am Soc Echocardiogr* 2009;22:1302-1308.
- (114) Zabalgoitia M, Ismaeil MF, Anderson L, Maklady FA. Prevalence of diastolic dysfunction in normotensive, asymptomatic patients with well-controlled type 2 diabetes mellitus. *Am J Cardiol* 2001;87:320-323.
- (115) Boyer JK, Thanigaraj S, Schechtman KB, Pérez JE. Prevalence of ventricular diastolic dysfunction in asymptomatic, normotensive patients with diabetes mellitus. *Am J Cardiol* 2004;93:870-875.
- (116) Fang ZY, Leano R, Marwick TH. Relationship between longitudinal and radial contractility in subclinical diabetic heart disease. *Clin Sci* 2004;106:53-60.
- (117) Fang ZY, Schull-Meade R, Downey M, Prins J, Marwick TH. Determinants of subclinical diabetic heart disease. *Diabetologia* 2005;48:394-402.
- (118) Gulati V, Katz W, Follansbee W, Gorcsan III J. Mitral annular descent velocity by tissue Doppler echocardiography as an index of global left ventricular function. *Am J Cardiol* 1996;77:979-984.
- (119) Delgado V, Mollema SA, Ypenburg C, Tops LF, van der Wall EE, Schalij MJ, Bax JJ. Relation Between Global Left Ventricular Longitudinal Strain Assessed with Novel Automated Function Imaging and Biplane Left Ventricular Ejection Fraction in Patients with Coronary Artery Disease. *J Am Soc Echocardiogr* 2008;21:1244-1250.
- (120) Greenberg NL, Firstenberg MS, Castro PL, Main M, Travaglini A, Odabashian JA, Drinko JK, Rodriguez LL, Thomas JD, Garcia MJ. Doppler-Derived Myocardial Systolic Strain Rate Is a Strong Index of Left Ventricular Contractility. *Circulation* 2002;105:99-105.
- (121) Vinereanu D, Nicolaidis E, Tweddel AC, Mädler CF, Holst B, Boden LE, Cinteza M, Rees AE, Fraser AG. Subclinical left ventricular dysfunction in asymptomatic patients with Type II diabetes mellitus, related to serum lipids and glycated haemoglobin. *Clin Sci* 2003;105:591-599.
- (122) Galderisi M, de Simone G, Innelli P, Turco A, Turco S, Capaldo B, Riccardi G, de Divitiis O. Impaired Inotropic Response in Type 2 Diabetes Mellitus: A Strain Rate Imaging Study. *Am J Hypertens* 2007;20:548-555.
- (123) Greenbaum RA, Ho SY, Gibson DG, Becker AE, Anderson RH. Left ventricular fibre architecture in man. *Br Heart J* 1981;45:248-263.

